Energy, Mines and Resources Canada | Énergie, Mines et Ressources Canada

CANMET

Canada Centre for Mineral and Energy Technology | Centre canadien de la technologie des minéraux et de l'énergie

HYDROGEN SULPHIDE CRACKING OF LINEPIPES: FINAL REPORT

G.J. BIEFER and M.J. FICHERA
CORROSION SCIENCE SECTION

AUGUST, 1984

ENERGY RESEARCH PROGRAM

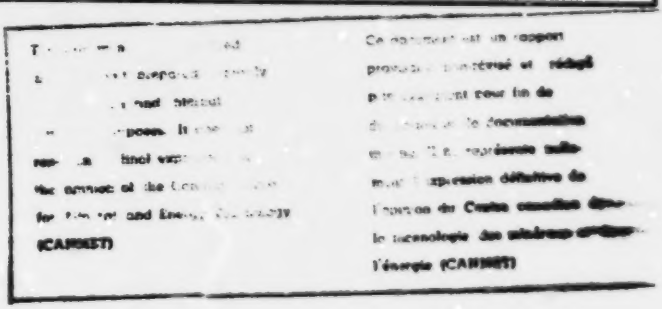

81 pf

PHYSICAL METALLURGY RESEARCH LABORATORIES
REPORT: ERP/PMRL 84-13(TR)

NOV 22 1984
MICROMEDIA

PHYSICAL METALLURGY RESEARCH LABORATORY
REPORT ERP/PMRL 84-13(TR)

HYDROGEN SULPHIDE CRACKING OF LINEPIPES: FINAL REPORT

by

G.J. Biefer and M.J. Fichera

EXECUTIVE SUMMARY

In a research program jointly sponsored by NOVA, Petro-Canada, Interprovincial Steel and Pipe Company, and Shell Resources Canada, nine gas transmission pipes were tested for sulphide stress cracking (SCC) and stepwise cracking (SWC) in order to rank the steels according to susceptibility, evaluate current NACE test methods, and shed some light on the failure mechanisms. The results show:

1. The SSC test is generally satisfactory, and results should be relevant to performance of sour gas linepipes at operating pressures. Improvements to pH control of the test solution and possibly shortening the maximum time of the test would be useful.
2. Increased susceptibility to SSC was shown in weld heat-affected zones and in the lower yield strength pipes tested.
3. The SWC test can identify steels resistant to specified H_2S environments but cannot always establish credible rankings according to susceptibility. Evaluation of SWC by ultrasonic C-scan is far more rapid and informative than the metallographic method specified. Test results should be relevant to sour-gas pipe performance at low pressures but their significance with respect to highly pressurized pipes is uncertain.

4. Susceptibility to SWC increased with increasing pipe yield strength, and in an aggressive acid H_2S environment, SWC was a maxiumum at temperatures below 15°C. SWC susceptibility was shown to correlate with size, spacing and distribution of inclusions in the pipe steels.

Suggestions for future research have been made, and include:

1. Investigation of the effect of temperature on the threshold stress for SSC, use of a more stable test solution, and shortening the test time. Further testing should evaluate the variation of SSC susceptibility with location in the pipe circumference and thickness, and determine whether there is a threshold concentration of dissolved hydrogen in the steel for SSC to occur.
2. Investigation of alternative methods of measuring SWC susceptibility by (i) determining critical hydrogen concentration in the steel for SWC; (ii) using permeation through pipe wall-thickness diaphragms to determine critical hydrogen fluxes for SWC. Further development of standard ultrasonic C-scan techniques is needed.
3. Research on SSC and SWC should concentrate on those classes of pipes most likely to be used to transmit sour hydrocarbons, i.e., oil country tubular goods and field gathering lines.

LABORATOIRE DE LA MÉTALLURGIE PHYSIQUE
RAPPORT ERP/PMRL 84-13(TR)

RAPPORT DÉFINITIF SUR LA FISSURATION DES CANALISATIONS CAUSÉE PAR LE SULFURE D'HYDROGÈNE

de

G.J. Biefer et M.J. Fichera

RÉSUMÉ POUR LA DIRECTION

Dans le cadre d'un programme de recherche parrainé par les sociétés NOVA, Petro-Canada, Interprovincial Steel and Pipe Company et Shell Resources Canada, le laboratoire a fait l'essai de la résistance de neuf canalisations de transport de gaz à la fissuration sous tension en milieu H_2S et à la fissuration en gradins, afin de classer les aciers selon leur susceptibilité, d'évaluer les méthodes d'essai actuellement utilisées par la NACE et d'expliquer les mécanismes de rupture. Voici les résultats obtenus:

1. L'essai de résistance à la fissuration sous tension en milieu H_2S est en règle générale satisfaisant; les résultats devraient donc bien témoigner du rendement des canalisations de transport de gaz riche en H_2S utilisées à des pressions normales. Il serait peut-être bon cependant de garder plus constant le taux d'acidité de la solution d'essai et peut-être aussi de réduire la durée maximale du test.
2. La zone de la soudure thermiquement affectée et les tuyaux de moindre résistance sont plus susceptibles de fissurer sous tension en milieu H_2S.
3. L'épreuve de fissuration en gradins permet de déceler les aciers qui résistent à certaines concentrations de H_2S mais elle ne permet pas toujours de leur attribuer un rang crédible selon leur susceptibilité. L'investigation des fissures par ultrasons est beaucoup plus rapide et plus utile que la méthode métallographique prescrite. Les résultats de cette méthode d'essai devraient donner une bonne idée du rendement des canalisations utilisées pour le transport de gaz riche en H_2S à faible

pression. Cependant, leur utilité est incertaine lorsque le transport s'effectue à des pressions élevées.

4 La susceptibilité à la fissuration en gradins croît proportionnellement à la tension de fluage du matériel. De plus, la fissuration atteint son maximum lorsque la température est inférieure à 15°C, en milieu très acide de H_2S. Il est démontré, qu'il existe un rapport entre la susceptibilité à la fissuration en gradins et les dimensions, l'espacement et la répartition des inclusions dans les aciers.

Parmi les points qui méritent plus de recherche, citons:

1 L'étude de l'effet de la température sur la contrainte limite pour la fissuration en milieu H_2S, l'utilisation d'une solution d'essai plus stable et une diminution de la durée de l'essai. Les autres recherches devraient porter sur l'évaluation de la variation de la susceptibilité à la fissuration causée par le H_2S selon sa situation dans la circonférence et l'épaisseur du tuyau, et déterminer s'il existe une concentration minimale d'hydrogène dissout dans l'acier qui permet cette fissuration.

2. Trouver d'autres méthodes de mesure de la susceptibilité à la fissuration en gradins 1) en déterminant le seuil critique de concentration d'hydrogène dans l'acier auquel se produit la fissuration; 2) en ayant recours à la perméation au moyen de diaphragmes de même épaisseur que les parois de la canalisation pour déterminer les fluxs critiques d'hydrogène. Les techniques ultrasoniques courantes ont aussi besoin d'être améliorées.

3. La recherche devrait surtout porter sur les catégories de canalisations qui conviennent le mieux au transport d'hydrocarbures riche en H_2S, c'est-à-dire les conduits de collecte au gisement et les fournitures tubulaires pour puits de pétrole.

INTRODUCTION

HISTORY OF THE H_2S CRACKING PROBLEM

Wet H_2S is acidic and corrodes steel, charging it with hydrogen that can cause cracking and blistering. H_2S-induced cracking failures of pipelines, tubing and other steel structures used in "sour" (wet H_2S) systems have been reported since the nineteen-fifties. In terms of established and simple tests, hardness was identified as the main factor correlated with failures of steel under tensile stress - denoted "sulphide stress cracking" (SSC) - and the National Association of Corrosion Engineers (NACE) cited HRC 22 as the maximum hardness compatible with acceptable resistance to SSC. Currently, purchases of pipe for anticipated sour environments specify this hardness limitation.

However, there have been occasional unexpected H_2S-induced cracking failures of pipelines with hardness values well below HRC 22 since the nineteen-fifties. These failures exhibited crack morphology differing from that shown in classical SSC, i.e., cracks initiate on the exposed surface and propagate transverse to the applied tensile stress (Fig. 1). Instead, the pipe walls developed internal cracks and surface blisters, the cracks predominantly in the plate rolling plane with occasional branching in the through-thickness direction. In some cases, a steplike crack group penetrated through a large fraction of the pipe wall, and this feature led to the use of the term "stepwise cracking" (SWC) by many researchers (Fig. 1).

CURRENT SSC AND SWC TESTS

The NACE has developed standard tests TM-01-77 and TM-02-84 to determine the susceptibility of steels to SSC and SWC respectively. The SSC test involves exposing a stressed specimen to an H_2S-saturated solution and determining the threshold tensile stress for resistance to SSC. In the SWC test rectangular coupons free from externally applied stress are immersed in H_2S-saturated synthetic seawater for a prescribed period. The amount of internal cracking and its orientation is subsequently assessed by examining metallographic sections.

Sour gas and oil fields are being exploited to an increasing extent, yet the NACE standard tests have seldom been used to assess the susceptibility to SSC and SWC of pipes manufactured in Canada. Furthermore, there is considerable skepticism about the applicability of experimental data from the NACE tests to service performance.

RESEARCH AT PMRL

In 1980 PMRL proposed research on the H_2S-induced cracking of linepipe steels (1). The program included a survey of the literature on SWC (2) and evaluations of SSC and SWC susceptibility of a number of linepipes, mostly of Canadian manufacture, using NACE standard tests. Test methods were to be assessed and cracking mechanisms defined to the extent possible. Recognizing the importance of work in this area, four Canadian companies NOVA, an Alberta corporation, Interprovincial Steel and Pipe Company, PetroCanada and Shell Canada Resources - agreed to provide partial funding at the rate of $10,000 per year from each company for a period of three years.

Research on the H_2S-induced cracking of linepipes has now been completed and the present report summarizes the results obtained from 1980-84. For clarity, detailed discussions are avoided in the body of the report and the reader is referred to References 1 to 10 and Appendices 1 and 2 for further details.

SUMMARY OF IMPORTANT RESULTS

Some of the characteristics differentiating SSC and SWC have been described in the introduction. The most important results in the research at PMRL from 1980-84 are as follows.

SULPHIDE STRESS CRACKING (SSC)

1. Consistent behaviour was exhibited in NACE standard SSC tests of tensile specimens in H_2S-saturated 5% sodium chloride - 0.5% acetic acid often called the "NACE solution". Parent and weld specimens from nine gas transmission pipes (Grades 290-483) yielded credible values of the threshold stress (THS) for resistance to SSC, given in Table 1 (3,4).
2. The ratio THS/YS is a measure of intrinsic SSC resistance, and values obtained in this research are plotted against YS in Fig. 2. THS/YS in parent SSC specimens increases with increasing YS of the pipe (3,4).
3. SSC specimens containing the weld usually failed in the HAZ as shown in Table 1. Figure 2 shows that THS/YS for weld specimens was generally lower than for parent specimens and independent of YS (3,4).

4. Parent SSC specimens taken 180° from the weld showed significant differences in THS values and mechanical properties from parent SSC specimens taken near the weld (Appendix 1).
5. During standard tests in H_2S-saturated solution SSC, specimens often developed significant internal cracking. This was evaluated using SWC test methods, and cracking ratios (%CTR) for the 9 pipes tested, measured on unbroken parent SSC specimens after 720 h at the THS, are given in Fig. 3. It shows that SWC is more likely to occur in stressed SSC specimens of lower strength pipes and can exceed the SWC determined on unstressed coupons from the same pipes in the standard SWC test (Appendix 1).
6. Fracture surfaces of SSC specimens were examined by scanning electron microscope (SEM). The most frequently observed fracture mechanisms were quasi-cleavage and microvoid coalescence. A few of the pipes showed intergranular cracking or numerous cleavage facets (Appendix 1).
7. Corrosion of SSC specimens during the NACE standard test caused a depletion of hydrogen ions in the test solution shown by increases in pH from initial values of 2.8 to final values as high as 4.6 (3).

STEPWISE CRACKING (SWC)

1. A survey of the technical literature on SWC has been published, covering test methods, and the effects of environmental, metallurgical and stress variables (2).
2. The NACE standard SWC test was performed in triplicate on ca 200 g rectangular coupons from nine gas transmission pipes (Grades 290-483). The coupons were free of external stress while immersed in one of two H_2S-saturated solutions for 4 days ("B.P.", synthetic seawater, ca 5.2 pH; "NACE", as in SSC test, ca 3.5 pH). After this, the amount of SWC was determined by measuring cracks on metallographic sections of the tested coupons. Figure 4 shows that reproducibility in the measurements was only fair, because of the uneven distribution of SWC-prone regions in the pipes (4,10).
3. SWC susceptibility of the nine pipes in terms of average %CTR is given in Tables 2 and 3. Tests carried out in the B.P. solution showed the differences between the pipes more clearly than those done in the more severe NACE solution (4,7).

4. Tests in the B.P. solution generally showed least susceptibility to SWC in parent metal adjacent to (0° from) the weld, and greatest susceptibility 180° from the weld (Table 2). But two pipes manufactured completely from remelted scrap showed a reverse trend (4,7).
5. There is a general trend towards increased SWC with increasing yield strength (4,7), as shown in Fig. 5 (4,7).
6. The volume of hydrogen absorbed by test coupons taken from the same pipe location correlated with SWC damage evaluated by metallography (Fig. 6). However, coupons from different pipes showed considerable variation in %CTR for the same amount by hydrogen absorbed (4,7,9).
7. Some coupons tested were evaluated for SWC by means of an ultrasonic C-scan (10). The ultrasonic beam, penetrating in the plate through-thickness direction, detected and displayed the uppermost areas of SWC in images such as those shown in Fig. 7. This provided a rapid and effective method of screening steels for their susceptibility to SWC.
8. Unexpectedly, SSC was observed in the coarse-grained heat-affected zone of a few weld SWC coupons of the higher strength pipes (Fig. 8). Microhardness traverses across the HAZ showed equivalent readings well above HRC 22, and it is assumed that residual tensile stresses were present. Weld coupons from other pipes, not showing SSC, had hardnesses below HRC 22 (4,7).
9. Coupons from a Grade 359 pipe were given standard SWC tests in the severe H_2S-saturated NACE solution at temperatures from 0 to 60°C. Metallographic evaluations of SWC showed considerable scatter and little effect of temperature in the range 15 to 60°C. At 0 and 5°C, higher %CTR values indicated more severe conditions than observed at 15 to 60°C (Appendix 1).
10. Length of elongated inclusions and groups of inclusions in the nine pipes studied were determined at PMRL, with a microstructure image analyzer. It was found that for six of the pipes total "inclusion length" correlated with total SWC crack length measured on tested coupons. The large deviations shown by three of the pipes were due to other microstructural factors having a strong effect on SWC (Appendix 2).

DISCUSSION

SULPHIDE STRESS CRACKING TEST

The NACE standard SSC test TM-01-77 was acceptable in that similar specimens exhibited consistent behaviour, and a well-defined THS - the threshold stress for resistance to sulphide stress cracking. Nevertheless, the research directed attention towards possible sources of error which are discussed in the following paragraphs.

1. Test solution

The H_2S-saturated NACE test solution has an initial pH value of 2.9, but corrosion of the SSC specimen always caused an increase in pH - to a value as high as 4.6 for a parent specimen of pipe Z, unfailed after 720 h (3). Thus, during tests, the aggressivity of the solution decreases with time - to a different extent with alloys showing different corrosion behaviour.

It is, therefore, difficult to determine the significance of some observations. Cracks in a specimen, unfailed after 720 h on test, might indicate that failure would have occurred had the test been extended. On the other hand, the cracks might have begun to propagate in the highly aggressive solution typical of the initial stages of testing, only to be deactivated as the pH increased in later stages of testing.

Comparisons between different steels would be more significant if solution properties could be held more constant during tests. With the NACE solution, this might be achieved by replenishment during tests and/or by greatly increasing the ratio:solution volume/specimen area. The development of an alternative test solution with better buffering characteristics would be a more convenient approach. Ikeda et al have reported improved pH stability in a solution of 5% NaCl - 0.75% $CH_3COONa.3H_2O$-0.5% CH_3COOH at a pH of about 4.3 (11).

2. Test duration

From an operational viewpoint, the 720 h run-out time specified by TM-01-77 is inconveniently long.

Figure 9 shows the frequency distribution of times-to-failure in standard SSC tests on 57 parent and weld SSC specimens in the present

research. Eighty-six per cent of the failures occurred at times of 100 h or less. Without making any other changes to TM-01-77, the use of a run-out period as short as one week could be considered. A run-out period of two weeks would exclude only one of the 57 failures recorded in our SSC tests i.e., only one of the THS values would have been changed (7).

The use of a more stable test solution, as discussed above, might increase the percentage of SSC specimens failing after relatively short exposures.

3. Specimen location in pipe

Our initial evaluation of SSC susceptibility of parent and weld specimens from 9 pipes showed that the weld HAZ was generally the microstructure most vulnerable to failure by SSC. It was concluded that the HAZ should be the focus of attention in pipe evaluations, and in attempts to develop more SSC-resistant pipe.

In SSC tests comparing parent metal 0° and 180° from the mill weld, pipes AE and CB showed unexpectedly larger values of THS and the ratio THS/YS in metal 180° from the weld, without a corresponding increase in YS. These results do not minimize the primary importance of the HAZ, but they do suggest that more testing should be performed (as in the evaluation of SWC susceptibility) to determine how SSC resistance can be expected to vary around a pipe circumference and the mechanisms involved (Appendix 1).

A disadvantage of SSC test TM-01-77 is that the 6.4 mm diam standard specimens can only represent a particular location of the metal in thicker-walled pipes - generally the centre-thickness. This location will not necessarily have the same susceptibility of initiation and propagation as metal at the pipe inner surface, which is in direct contact with the sour environment. For a few thick-walled pipes, it would be useful to compare the SSC behaviour of "surface" and "centre-thickness" specimens.

STEPWISE CRACKING TEST

The NACE standard SWC test TM-02-84 codifies procedures that have been found useful for some years (2,4,11,12). Our research shows that the test is capable of identifying steels resistant to specified H_2S environments, but cannot always provide a credible ranking of their susceptibility to SWC. A more detailed discussion follows.

1. Metallographic evaluation of SWC

The standard SWC test is simple and straight-forward insofar as fabrication, preparation and hydrogen-charging of test coupons is concerned. Most of the equipment required is standard in any metallographic laboratory. However, difficulties arise in the quantitative evaluation of SWC by the detection and measurement of cracks in metallographic sections. This process is inordinately time-consuming, to some extent subjective, and requires a skillful, conscientious operator.

There is a more serious basic drawback to metallographic evaluations arising from the nature of the cracking examined. SWC is usually unevenly distributed, in groups of varying shape and size some comparatively large such that the three metallographic sections specified at each of 3 locations in the pipe circumference are often too small a sample to represent adequately the SWC in the pipe as a whole.

This is shown in our research, in which all SWC tests were run in triplicate; reproducibility between coupons from the same part of a pipe was only fair. Averaging the results from 3 coupons at each of 3 locations yielded a more credible result than the single coupon specified in the standard trst but consumed too much operator time to be considered as normal practice (4,7).

If many steels must be examined, a more rapid and simple method of evaluating SWC is needed representative of a much larger volume of metal.

2. Test temperature

The effect of temperature on SWC was investigated by Japanese researchers using H_2S-saturated synthetic seawater as the test solution, and their results indicate that temperature changes between 15° and 35°C have little effect on SWC (2). This justified the choice of a temperature of 25 ± 3°C in the NACE standard SWC test, in which synthetic seawater is specified as the test solution.

In the present research, the effect of temperature upon SWC was investigated in the more severe NACE solution. There were no indications of temperature changes in the range 15° - 60°C causing an effect on SWC and therefore nothing against the choice of 25 ± 3°C as the standard test temperature (Appendix 1).

3. Flattening of pipe wall

The flattening of pipe wall is permitted in the standard SWC test in order to facilitate the machining of test coupons. However, the literature indicated that cold working might have a significant effect on SWC susceptibility (2).

Comparative SWC tests on flattened and non-flattened coupons in the B.P. and NACE solutions yielded cracking ratios within the normal scatter band, indicating no detectable effect from the flattening. On the other hand, the occurrence of SSC in hard HAZs in some weld coupons suggests that flattening might have generated the requisite tensile residual stresses (7).

It should be kept in mind that flattening of the pipe wall might, in some cases, affect the results of SWC tests - in which case, non-flattened specimens should be used.

4. Measurement of cracking ratio

In NACE Standard TM-02-84, the crack length ratio is defined by,

$$CLR = \sum_i \frac{\ell_i}{L} 100\%$$

Here ℓ_i = the length of a particular internal crack and L = 2 cm - i.e., the width of the standard test coupon (Fig. 1, Appendix 1).

Consideration of the above reveals that the CLR, unlike the other two ratios CTR and CSR, is a function of coupon thickness T. All else being equal, the CLR will increase with increasing T, and comparisons of SWC susceptibility in terms of CLR are only valid for coupons having the same thickness.

To eliminate the effect of coupon thickness, SWC crack length ratios may be expressed in terms of concentration per unit area, i.e.,

$$\%CLR/cm^2 = \sum_i \frac{\ell_i \, 100\%}{L\,(TL)}$$

Here T is the test coupon thickness in cm.

The NACE Standard, published in 1984, excludes from the calculations of cracking ratios all cracks lying entirely within 1 mm of the inside or outside surface of the test coupon. At PMRL, cracks on the entire surface were counted, in accordance with the draft of the SWC test available in 1980.

ALTERNATIVES TO STANDARD SWC TEST

1. Diffusible hydrogen at 45°C

Determination of the volume of hydrogen absorbed by a coupon during a SWC test is a relatively simple procedure, and many researchers have reported a correlation between absorbed hydrogen and the amount of SWC (2). Since the entire ca 200 g coupon is being sampled, absorbed hydrogen can in principle provide a more valid estimate of susceptibility to SWC than the small slices used in metallographic evaluations.

In the present work, absorbed hydrogen was shown to correlate with SWC damage, as determined by metallography; in some measurements reproducibility of hydrogen contents was superior to that of SWC cracking ratios (Appendix 1). However, correlation was obtained only if the measurements were restricted to one steel, because some steels absorbed very different amounts of hydrogen in association with a unit of SWC damage (Fig. 6). Absorbed hydrogen was, therefore, unsuitable as a general index to compare SWC susceptibilities of different pipes.

Despite the above limitation, "diffusible hydrogen at 45°C" could be useful in quality control or in laboratory tests where the effect of varying some parameter on SWC e.g., temperature or H_2S concentration is being examined on only one alloy.

It has been reported that there is a consistent error in the collection of hydrogen gas by displacement of glycerol at 45°C. Ito et al compared glycerol and mercury in gas collectors, and developed a formula for conversion of hydrogen volumes obtained in glycerol to the more accurate volumes which would be obtained in mercury (13).

Mercury was avoided in the research at PMRL because of its toxicity, and the uncorrected values obtained using non-toxic glycerol were reported. Savage and Nippes have developed a method for the determination of diffusible hydrogen by collection from non-toxic silicone oil at 100°C, and report that results are similar to those using mercury (14). In the present work, silicone oil was tried at 45°C and found to be ineffective, apparently because of dissolution of the hydrogen gas at this temperature. Investigation of silicone oil at 100°C is recommended.

2. Ultrasonic C-scan

The principal disadvantages of the metallographic evaluation of SWC, discussed above, may be overcome by using an ultrasonic C-scan. In our work, an ultrasonic beam scanned one of the major coupon surfaces, penetrating in the through-thickness direction. It provided a rapid and direct indication of the uppermost areas containing SWC, as shown in Fig. 7 (7,10). An image analyser was used to express the results quantitatively in terms of % coverage by SWC.

There are evidently difficulties in the precise interpretation of images provided by the C-scan, and a few anomalous indications required verification. In our measurements, through-thickness cracks were undetectable; severe SWC would be underestimated because overlapping cracks were recorded as single cracks. At present, there is no accepted standard method of using the C-scan in evaluating SWC. But of the three methods of evaluation examined, the C-scan was by far superior with respect to speed and the amount of information provided, and it appears well adapted to comparing SWC susceptibilities of different steels.

A possible disadvantage, compared with evaluations of SWC by metallography and by absorbed hydrogen, is the necessity to procure, maintain and operate expensive, highly sophisticated equipment.

3. Measurement of C_{th}

Beyond the experimental difficulties discussed above, the standard SWC test can be criticized for its arbitrary character. Linepipe steels are rated in terms of the SWC damage caused by 4 days immersion in a specified H_2S-saturated solution. But there is no fundamental reason for the choice of these particular conditions and the resulting SWC ratios can only be related on an ad hoc basis to the behaviour of the same steels in sour service.

Ikeda et al have shown that there is a critical concentration of dissolved hydrogen in a steel, termed C_{th}, that must be attained before SWC can occur. Values of C_{th} might be 0.3 to 0.4 mL (STP)/100 g for an ordinary steel, highly susceptible to SWC, but over 2.5 mL (STP)/100 g for a highly resistant Ca-deoxidized steel (11).

Provided that convenient methods for its determination can be developed, the use of the C_{th} of a steel as a measure of its resistance to SWC would be a far more rational approach than that used in the present NACE standard test. There would be less difficulty in ranking steels in their susceptibility to SWC; even more important, the C_{th} value of a steel can be related directly to the performance of that steel in a transmission pipe containing a corrosive sour environment. In such a pipe, permeation methods can be used in the field to determine the maximum concentration of dissolved hydrogen in the wall C_o; SWC should only occur when $C_o \geq C_{th}$.

4. Measurement of critical hydrogen flux

By using relatively large diaphragms of full pipe wall thickness, permeation methods alone are in principle capable of providing a direct and precise index of susceptibility to SWC. Techniques would have to be developed for permeating hydrogen through the diaphragm at a constant flux then increasing the flux by increments until SWC was detected - whether by changes in permeation kinetics, by ultrasonic C-scan, or by using an acoustic emission probe. The parameter indicative of SWC resistance of a pipe wall would be the lowest hydrogen flux causing SWC damage - i.e the "critical hydrogen flux". The value of this parameter determined in the laboratory should be directly applicable to the same pipe, transporting sour gas, in the field.

GENERAL

Relationship of SSC AND SWC

Tests on unstressed coupons show that SWC cracking ratios increase with the yield strength of the pipe (Fig. 5). But SSC resistance also increases with yield strength (Fig. 2). This leads to the parodoxical result that SSC resistance (as THS/YS) increases with internal cracking (as %CTR), as shown in the poorly defined linear relationship of Fig. 10. However, Fig. 10 does not necessarily provide any relevant information regarding SSC mechanism, because there is no assurance that SWC behaviour observed in an unstressed coupon will be related in a systematic way to SWC behaviour in a tensile stress field.

In classical SSC, cracks initiate at the surface of the specimen and propagate transverse to the applied stress until the specimen fails. In the present research, gauge lengths of SSC specimens from all pipes developed surface cracks. But metallographic sections of the gauge lengths of unfailed SSC specimens also showed internal cracking of the type denoted SWC in most of the pipes (Appendix 1).

From a superficial examination of the fractured SSC specimens it was not clear whether the surface cracks had propagated to an "SSC failure" (by trans- and/or inter-granular cracking), or whether internal SWC had weakened the specimens to the point of "SWC failure". However, the results of the examinations of tested SSC specimens (Appendix 1) permitted a tentative answer to this question. The relevant observations are given in Table 4 with respect to parent metal SSC specimens only, to avoid the microstructural complexities of weldments.

Growth of SWC, the development of transverse crack groups, and marked delamination in the rolling plane at the THS are manifestations of SWC - especially when the alternatives of cleavage (transgranular cracking) and intergranular cracking are absent - and this identifies AB, CA and CD as SWC failures. Conversely: AE, AG and CE show the cleavage and/or intergranular cracking characteristic of SSC failures, with nothing indicative of SWC.

CB shows SWC behaviour except for an absence of SWC growth; but its level of SWC was high to begin with. It is significant that the globular inclusions of CB were lined up to give the highest average length of inclusion groups of the nine steels (Appendix 2). CC resembled AE and exhibited SSC behaviour except for the presence of SWC growth; but there was not much growth. The behaviour of Z was the most ambiguous of the 9 steels but it is tentatively assumed to have failed by SSC.

A direct correlation between the results of standard SSC and SWC tests might be expected if (i) SWC showed a definite relationship to tensile stress; and (ii) failures of SSC specimens all showed SWC as the dominant mechanism. The present work, though not conclusive, contradicted both assumptions. The inverse relationship of Fig. 10 notwithstanding, it is concluded that there is no significant mechanistic relationship between the results of standard SSC and standard SWC tests.

Significance of standard SWC test

Data from the standard SWC test will indicate the tendency of a pipe carrying a sour hydrocarbon to develop internal cracking at low or atmospheric pressure - e.g., at start-up or shut-down. It will often be possible to rank pipe materials, to ensure to the extent practicable that the pipe most resistant to SWC is being used. As discussed above, our research indicates that data from unstressed SWC coupons cannot predict H_2S-induced cracking behaviour in sour pipe at high operating pressure - i.e., under a relatively high tensile stress - because SSC may supersede SWC.

SWC can only occur in an operating sour-gas pipeline if the maximum hydrogen concentration C_o in the pipe wall equals or exceeds C_{th}, the critical hydrogen concentration for SWC. At present, SWC does not seem to be a problem in sour-gas pipes in Canada and it is probable that the combined material susceptibility and environmental severity required to cause SWC are rarely attained.

Significance of standard SSC test

Data from standard SSC tests will be relevant to the cracking behaviour of pressurized sour-gas pipes, whether the dominant mechanism is SSC or SWC. The main problems with the test are that the entire plate thickness is not tested, and that corrosion of an SSC specimen in a limited volume of test solution causes changes in the severity of the test solution. The SSC test specimen can provide values of the threshold stress THS, and also of SWC cracking ratios as a function of applied stress; it can, therefore, provide much more information than unstressed SWC coupons.

Linepipes are most susceptible to SSC in the HAZ of the weld; it is, therefore, vital to test SSC specimens containing the weld in evaluating the SSC-resistance of a pipe.

Relevance of results to pipeline field experience

As discussed above, both the NACE standard SSC and standard SWC tests are valuable in assessing the resistance of pipe material to H_2S-induced cracking.

Some of the steels studied at PMRL are unlikely to be exposed to sour environments. In particular AB, AE, AG, CC and Z are large diameter high strength pipes that would be installed as main transmission lines. Gas being transmitted in these lines has been cleaned and only an equipment breakdown would result in exposure to wet H_2S. The main areas where wet-H_2S is a problem are in oil country tubular goods and field gathering lines. Pipes CE, CA and CB are likely to find use as field gathering lines. The importance of wet H_2S and CO_2 attack on oil country tubular goods will be addressed in new research now being initiated at PMRL.

CONCLUSIONS

SSC test

1. The standard SSC test provided credible values of the threshold stress THS for each of the pipes. The results given by the test are in principle relevant to the service performance of pipelines transporting a sour product at operating pressures.
2. Weld-containing specimens were generally less resistant to SSC than parent metal specimens, and usually failed in the HAZ. This zone should be the focus of attention in attempts to develop more SSC-resistant pipes.
3. In parent metal, the ratio THS/YS, an index of intrinsic resistance to SSC, was observed to increase with increasing yield strength over the range 368-643 MPa.

SWC test

1. The standard SWC test was capable of identifying steels resistant to specified H_2S environments, but could not always establish a credible ranking of SWC susceptibility. Results from SWC tests appear to be relevant to the performance of sour gas pipes at low or atmospheric pressure - e.g., at times of pipeline start-up and shutdowns. Their significance is uncertain with respect to the vital case of a highly pressurized sour-gas pipe.

2. Ultrasonic C-scan provided the most rapid and informative method for evaluating SWC in a test coupon, but standard procedures do not exist at present. Metallographic evaluations are time-consuming and poorly reproducible while measurements of "diffusible hydrogen 45°C" are only useful to a limited extent.
3. In standard tests on parent metal, susceptibility to SWC was observed to increase with increasing yield strength over the range 368-643 MPa.
4. Tests of the effect of temperature in the highly aggressive NACE solution showed similar susceptibility to SWC in the range 15-60°C. Below 15°C, increased susceptibility to SWC was indicated.

Relationship of SSC and SWC

1. There is no significant relationship between the results of NACE standard SWC and standard SSC tests.
2. Unstressed coupons of all nine pipes showed SWC; but on application of tensile stress, only four pipes with distinctly or slightly elongated inclusions or with very high susceptibility to SWC exhibited failures in which the dominant mechanism was SWC.
2. Stressed specimens from the five pipes which did not fail by SWC generally showed evidence of the transgranular or intergranular cracking characteristic of SSC.

RECOMMENDATIONS FOR FUTURE RESEARCH

1. The standard SCC test could be improved by developing a more stable test solution and adopting a much shorter run-out period than 30 days.
2. Tests should be performed to determine whether susceptibility to SSC is related to a critical concentration of dissolved hydrogen C_{th}.
3. SSC testing should be performed to determine the extent of the dependence of THS on the exact position of specimens around the pipe circumference, and through the pipe thickness.
4. The effect of temperature upon THS should be determined - no data are at present available.
5. Methods should be developed to assess SWC susceptibility in terms of the critical concentration of dissolved hydrogen, C_{th}. This parameter is of fundamental significance and may relate to SSC as well as SWC behaviour. It should be possible to use C_{th} data in predicting the danger of H_2S cracking of pipes in sour service.

6. Permeation tests should be performed on full wall-thickness diaphragms of linepipe steels to determine critical hydrogen fluxes for SWC damage. Such data should be applicable to pipes in sour service.
7. The effect of stress on SWC should be investigated in linepipe steels containing elongated inclusions which have been shown to fail by SWC in tension tests.

ACKNOWLEDGEMENTS

This research has been given partial financial support by the Interprovincial Steel and Pipe Company Ltd.; PetroCanada; Nova, an Alberta Corporation; and Shell Canada Resources Limited. The Steel Company of Canada provided some linepipe at no charge. Important assistance with the experimental work was given by J.C. Selwyn and S. Murray, formerly with the Corrosion Science Section, Physical Metallurgy Research Laboratories (PMRL). Alcan International Limited, Kingston, Ontario, generously made their ultrasonic C-scan facility available and provided technical assistance. The drawings and photographs were produced respectively by the PMRL Draughting and Photographic Services. Test specimens were made by the Technical Services Division of CANMET. Technical advice given by Dr. J.B. Gilmour, Head, Corrosion Science Section, and Dr. M.J. Godden, Project Leader, Pipelines, is greatly appreciated. Dr. V.S. Sastri of the Corrosion Science Section performed some hot-extraction hydrogen analyses.

REFERENCES

1. Biefer, G.J. "Hydrogen sulphide cracking of pipeline steels: status of the problem and proposal for research at PMRL"; Division Report ERP/PMRL 80-67(TR); CANMET, Energy, Mines and Resources Canada; 1980.

2. Biefer, G.J. "The stepwise cracking of pipeline steels in sour environments"; Mater Perform 21:6; 19-34; 1982.

3. Biefer, G.J. and Fichera, M. "Sulphide stress cracking tests on gas transmission linepipe"; Division Report ERP/PMRL 82-64(TR); CANMET, Energy, Mines and Resources Canada; 1982.

4. Biefer, G.J. and Fichera, M. "Sulphide stress cracking and stepwise cracking tests on gas transmissions linepipes"; Division Report ERP/PMRL 83-17(OP-J); CANMET, Energy, Mines and Resources Canada; 1983. In: Proc of Symp on Effect of Hydrogen Sulphide on Steel at 22nd Ann Conf Metallurg Can Inst Min Metallurg; Aug 22-24, 1983; Edmonton; 1-37; 1983.

5. Biefer, G.J., Fichera, M.J. and Selwyn, J. "Stepwise cracking tests of linepipe in H_2S environments"; Division Report ERP/PMRL 81-39(TR); CANMET, Energy, Mines and Resources Canada; 1981.

6. Fichera, M.J. "Procedure used for stepwise cracking research at PMRL"; Division Report ERP/PMRL 81-51(INT); CANMET, Energy, Mines and Resources Canada; 1981.

7. Biefer, G.J. and Fichera, M.J. "Evaluation of H_2S-induced stepwise cracking of linepipe"; Division Report ERP/PMRL 83-7(TR); CANMET, Energy, Mines and Resources Canada; 1983.

8. Biefer, G.J., Fichera, M. and Selwyn, J. "Stepwise cracking behaviour of some Canadian line pipes"; Canadian Metallurgical Quarterly 22:2; 225-233; 1983.

9. Selwyn, J.C. "Determination of diffusible hydrogen at 45°C in stepwise cracking measurements on linepipe steel"; Division Report ERP/PMRL 81-58(INT); CANMET, Energy, Mines and Resources Canada; 1981.

10. Mak, D.K. "Ultrasonic inspection of stepwise cracking"; Division Report ERP/PMRL 83-10(TR); CANMET, Energy, Mines and Resources Canada 1983.

11. Ikeda, A., Kaneko, T., Hashimoto, T., Takeyama, M., Sumitomo, Y. and Yamura, T. "Development of hydrogen induced cracking (HIC) resistant steels and HIC test methods for hydrogen sulphide service"; In: Proc of Symp on Effect of Hydrogen Sulphide on Steel, at 22nd Ann Conf Metallurg Can Inst Mining Metallurg; Aug 22-24, 1983; Edmonton; 1-71; 1983.

12. Moore, E.M. and Warga, J.J. "Factors influencing the hydrogen cracking sensitivity of pipeline steels"; Mater Perform 15:6:17-23; 1976.

13. Ito, Y., Nakanishi, M. and Komizo, Y. "Hydrogen delayed cracking in low alloy high strength steel weldment"; The Sumitomo Search; 22:11; 156-167; 1979.

14. Savage, W.F. and Nippes, E.F. "Development and qualification of methods for the determination of diffusible hydrogen content in weldments"; Interim Technical Report for the period July 1, 1977 to June 30, 1980, Contract No. N00014-75-C-0944, NR 031-780; U.S. Office of Naval Research; 1981.

15. Tanimura, M. "Private communication to NACE Task Group T-1F-20 - on visual inspection of NACE TM-01-77 test specimen"; Nippon Kokan K.K., Japan, September 1983.

16. Burns, D.S. "Laboratory test for evaluating alloys for H_2S service"; Materials Performance 16:9:9-15; 1977.

Table 1. Threshold stress for resistance to SSC and microstructures in which failure cracks occurred in weld specimens.

	Parent specimens		Weld specimens		
Pipe	THS* MPa	Ratio: THS / YS**	THS MPa	Ratio: THS / YS	Microstructure of failure crack
AB	348	0.67	410	0.70	HAZ, HAZ
AE	429	0.66	309	0.48	HAZ, HAZ
AG	545	0.91	343	0.61	HAZ, HAZ, WFZ
CA	269	0.64	269	0.62	HAZ, HAZ, HAZ
CB	336	0.68	269	0.53	HAZ, HAZ, HAZ, P, P
CC	317	0.60	436	0.74	HAZ, HAZ
CD	258	0.62	258	0.57	HAZ, HAZ, P, P
CE	235	0.64	206	0.55	HAZ, HAZ, HAZ
Z	459	0.85	314	0.51	HAZ, HAZ, HAZ

*THS = Threshold stress for resistance to SSC

**YS = Yield strength

Table 2. Average crack thickness ratio (%CTR) in triplicate tests in H_2S-saturated synthetic seawater (B.P. test).

		Parent metal		
Pipe	Weld HAZ(1)	0° from weld(2)	90° from weld(3)	180° from weld(3)
AB	11	5.2	2.4	2.3
AE	4.5	6.2	8.2	7.5
AG	11	7.6	0.1	0.7
CA	10	6.0	6.8	13
CB	0	1.4	9.8	17
CC	0	0.3	1.8	3.0
CD	0	0	0	0
CE	0	0	0	0.2
Z	0(4)	0	5.3	3.9

(1) based on 3 metallographic sections

(2) based on 6 metallographic sections

(3) based on 9 metallographic sections

(4) apparent SSC in coarse-grained HAZ of 1 metallographic section in which micro-hardness in weld HAZ was above HRC 22 equivalent (see text)

Table 3. Average crack thickness ratio (%CTR) in triplicate tests in H_2S-saturated NACE solution.

Pipe	Weld HAZ[1]	Parent metal		
		0° from weld[2]	90° from weld[3]	180° from weld[3]
AB	66	25	23	21
AE	16[4]	12	19	14
AG	18[4]	18	11	9.1
CA	88	17	18	19
CB	26	35	37	27
CC	15	14	11	6
CD	0	0.5	3.0	7.7
CE	0	0	1.0	0.5
Z	0	7.5	12	24

(1) based on 3 metallographic sections

(2) based on 6 metallographic sections

(3) based on 9 metallographic sections

(4) apparent SSC in coarse-grained HAZ of 1 metallographic section in which microhardness in weld HAZ was above HRC 22 equivalent (see text)

Table 4. Factors related to cracking behaviour of parent SSC specimens

Pipe	Specimen fracture surfaces show:						Failure mechanism in SSC tests
	SWC Growth at THS	Transverse crack groups at THS	Cleavage (CL)	Inter granular cracking (IG)	Marked delamination	Inclusion shape	
AB	Yes	Yes	-	-	Yes	elongated	SWC
AE	-	-	Yes	-	-	globular	SSC
AG	-	-	-	Yes*	-	globular	SSC
CA	Yes	Yes	-	-	Yes	elongated	SWC
CB	-	Yes	-	-	Yes	globular	SWC
CC	Yes	-	Yes	-	-	globular	SSC
CD	Yes	Yes	-	-	-	ellipsoidal	SWC
CE	-	-	-	Yes	-	globular	SSC
Z	-	-	-	-	-	globular	SSC

*Observed in metallographic section at the tip of a propagating crack

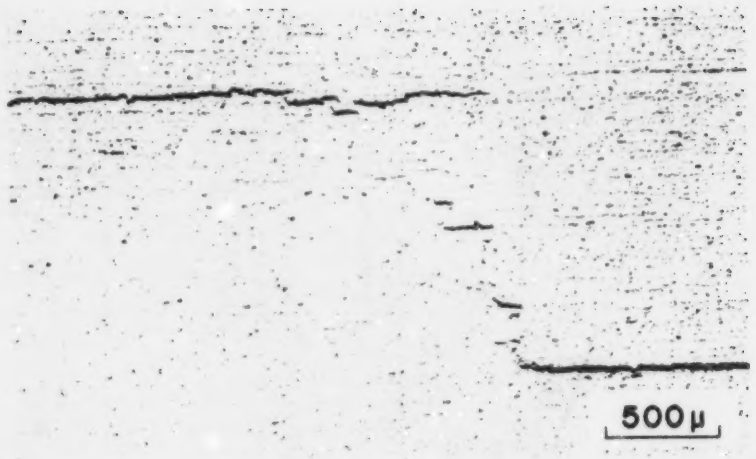

100X
410SS QTT 21-22 HRC
96.8 ksi 95% 2.0h

Fig. 1. Metallographic sections showing SSC (at left) (16) and SWC (at right) observed in parent metal of pipe CB in laboratory testing. (negs 3747 and 8038)

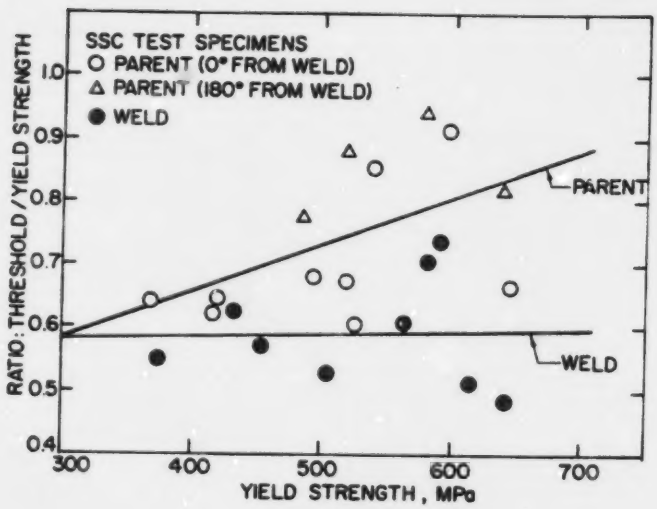

Fig. 2. Least squares plots of data from SSC tests in H_2-saturated NACE solution on parent and weld specimens of gas transmission pipes. (neg 10114)

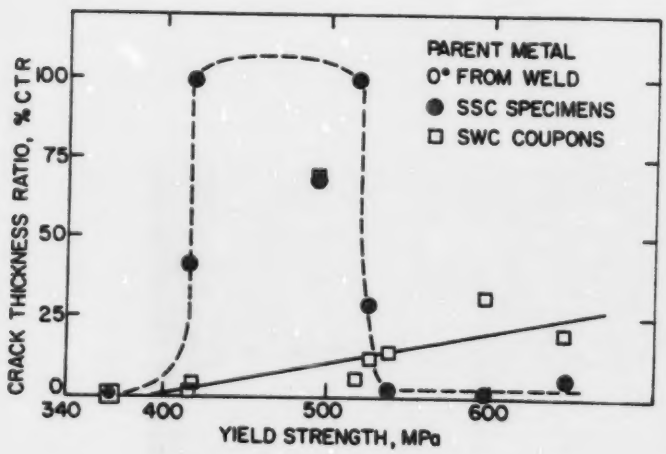

Fig. 3. %CTR values determined on (i) unfailed parent metal SSC specimens after testing at the threshold stress THS for 720 h and on (ii) unstressed SWC coupons - both plotted against SSC specimen yield strength. (neg 10120)

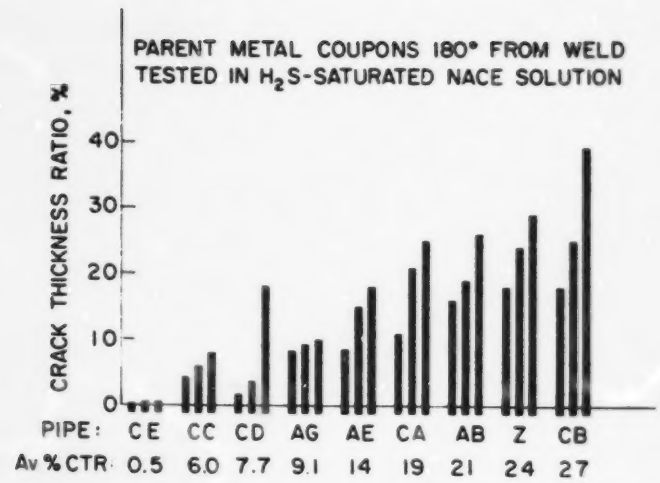
PARENT METAL COUPONS 180° FROM WELD
TESTED IN H_2S-SATURATED NACE SOLUTION
CRACK THICKNESS RATIO, %
0
10
20
30
40
PIPE: CE CC CD AG AE CA AB Z CB
Av %CTR 0.5 6.0 7.7 9.1 14 19 21 24 27

Fig. 4. %CTR values for individual SWC coupons of parent metal after testing in H_2S-saturated NACE solution. (neg 8091)

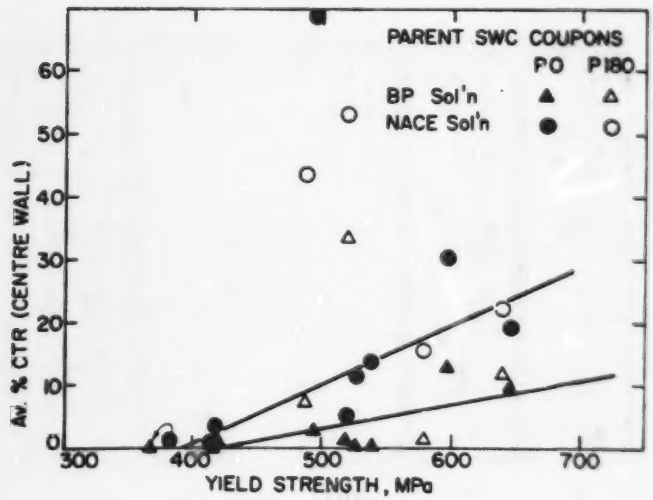

Fig. 5. Av %CTR from SWC measurements on coupons plotted against yield strength for the 9 linepipe steels tested. The lines are those given previously (4), based exclusively on parent metal 0° from the weld (P-0), and results obtained on metal 180° from the weld (P-180) are also included. (neg 10115)

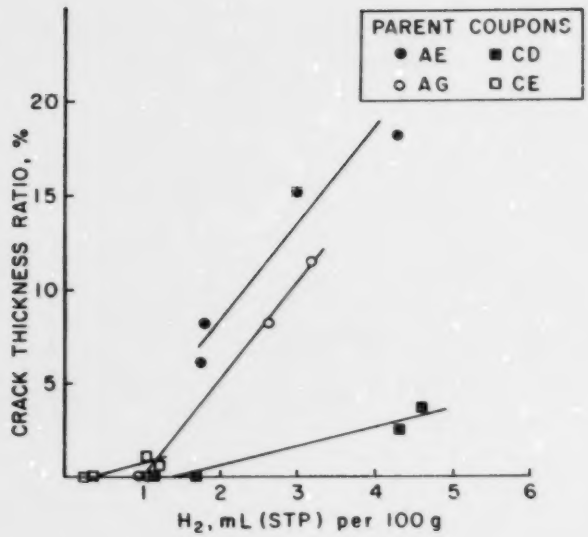

Fig. 6. Diffusible hydrogen at 45°C related to the crack thickness ratio %CTR for parent coupons of four pipes. (neg 7830)

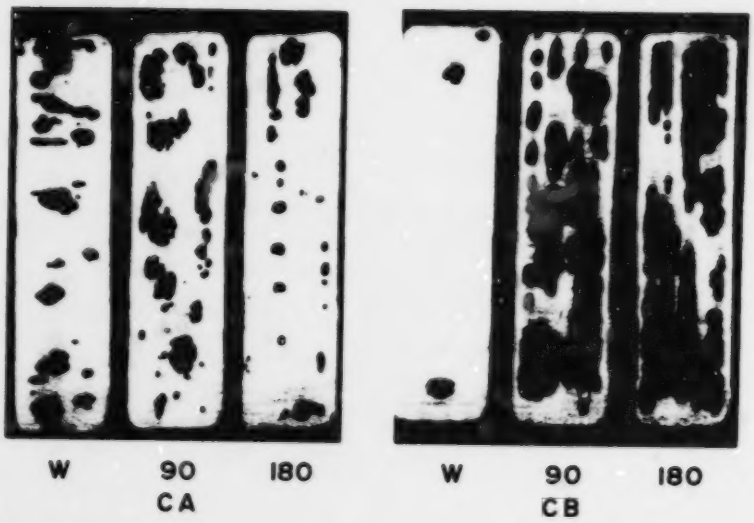

Fig. 7. Ultrasonic C-scan images of standard SWC coupons after testing in H_2S-saturated seawater. The well-defined dark areas represent SWC. (neg 7575)

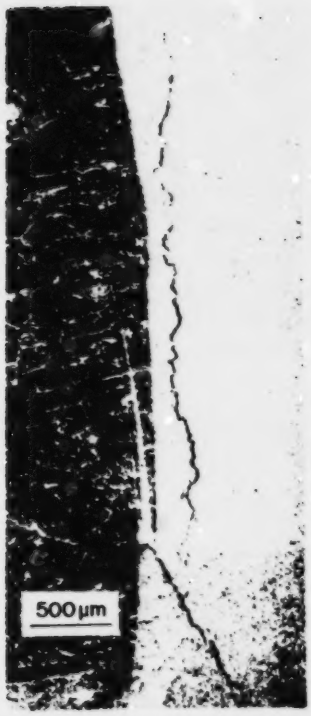

Fig. 8. SSC in the coarse-grained HAZ of a SWC weld coupon from pipe Z. (neg 10623)

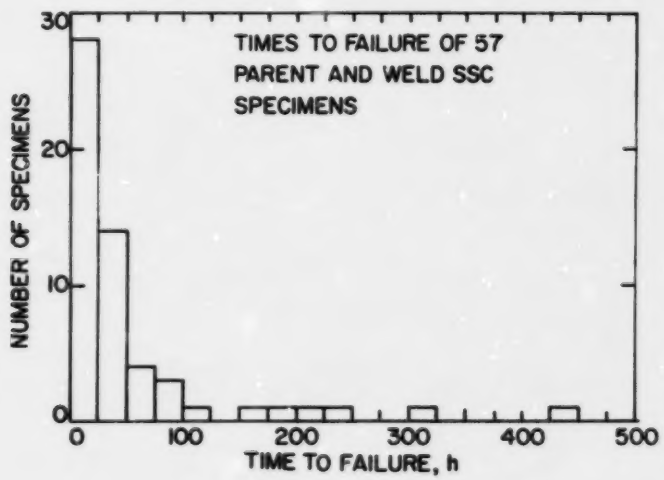

Fig. 9. Frequency distribution of times to failure in standard SSC tests of parent and weld specimens from nine gas distribution pipes. (neg 10116)

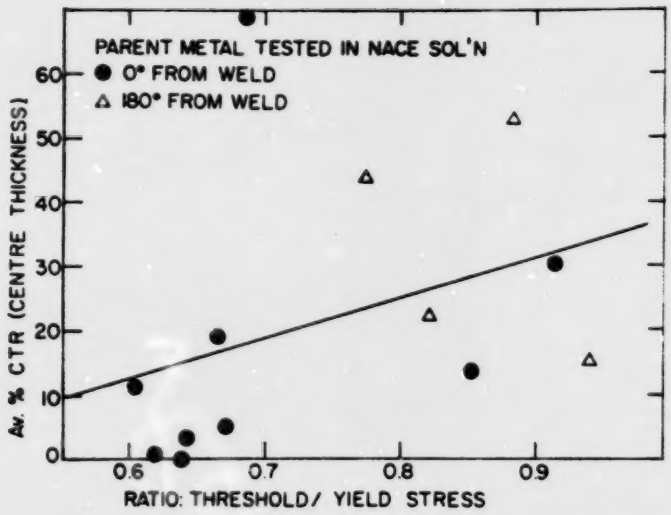

Fig. 10. Least-squares plot of %CTR (from tests on SWC coupons) ploted against ratios THS/YS obtained in SSC tests. (neg 10113)

APPENDIX 1

This appendix describes research completed after August 1983, and not reported elsewhere. Discussion of the work is in the body of this report.

SULPHIDE STRESS CRACKING

The NACE has developed standard test method TM-01-77 for evaluating the resistance of metals to SSC at ambient temperatures. Basically, the test consists of the exposure of metal specimens under tensile loading to 5% sodium chloride - 0.5% acetic acid solution saturated with H_2S (the NACE Solution). The time to failure is measured as a function of applied stress.

STANDARD SSC TESTS

At PMRL, test TM-01-77 was used to determine the "maximum threshold stress" for resistance to SSC (THS) on specimens from 9 gas transmission pipes. Tables 1 and 2 give the THS values determined for parent and weld specimens along with yield strengths (YS) and THS/YS ratios. THS/YS is a measure of intrinsic resistance to SSC.

The parent SSC specimens used in these tests were usually made from metal located near the mill weld (i.e., about 0° from the weld) and specimen lengths were transverse to the plate rolling direction. Metallographic sections of SSC specimens used to investigate internal cracking (SWC) and other features were always prepared on a plane normal to the rolling direction as shown in Fig. 1. The lengths of SSC specimens were parallel to the L dimension in this Figure. The weld SSC specimens contained the mill weld at the centre of the gauge length, and specimen lengths were transverse to the direction of the weld.

The ratios THS/YS obtained in the SSC measurements are plotted against YS in Fig. 2, which includes results for parent specimens 180° from the weld. For both parent and weld specimens, the data points show considerable scatter from the least squares lines. Parent metal ratios increase with increasing YS, and are generally larger than weld specimen ratios, which are independent of YS (1,2).

EXAMINATION OF SSC SPECIMENS

After the SSC test, the corroded surfaces of the gauge lengths of all specimens were examined by low-magnification stereomicroscopy. To determine the amount of internal cracking, metallographic sections of some of the unfailed SSC specimens were examined. Fracture surfaces of some of the specimens were inspected by the scanning electron microscope (SEM). In connection with the SEM measurements, additional metallographic sections were examined.

Gauge length surfaces

Specimens of all pipes showed surface pitting and grooving which was not characterized. In addition to this damage, and sometimes associated with it, were the four types of surface cracking shown schematically in Fig. 3. The principal types of cracking observed on each pipe are listed in Table 3.

Through-thickness (T) surface cracks were so positioned on the specimen circumference that tangents were approximately parallel to the plate rolling plane - i.e., crack propagation was predominantly in the plate through-thickness direction. As indicated in Table 3, T cracks were the most prevalent type. Small blisters (B) often occurred on the same part of the specimen circumference as the T cracks. Some of the blisters were cracked.

Side-cracks (S) were occasionally seen, approximately on the plane viewed in metallographic examinations (Fig. 1.); S cracks showed the characteristics of SWC. Circumferential (C) cracking of the type indicated in Fig. 3 and illustrated in Fig. 4 was observed only in specimens from pipe AG. It occurred in all parent metal specimens tested, with applied stress/YS ratios from 0.541 to 0.946. In view of the superior resistance to SSC shown by pipe AG, these C cracks were apparently <u>not</u> indicative of susceptibility to SSC (1,2).

There were approximately equal proportions of weld fusion zone (WFZ), heat affected zone (HAZ), and parent metal in gauge lengths of weld specimens. The test solution etched the three microstructures differentially, so that they could usually be distinguished. As shown in Table 4, weld specimens usually failed in the HAZ. There were also a few failures in parent metal, and one in the WFZ. Values of THS for the three microstructures in each pipe can, therefore, be ranked:

WFZ > parent > HAZ

Internal cracking (SWC)

Metallographic sections of the gauge lengths of tested SSC specimens often showed internal cracking, resembling that seen in SWC tests on unstressed coupons (2). In the present work, this internal cracking was measured quantitatively using the procedures of the NACE standard SWC test TM-02-84. The crack thickness ratio (%CTR) was usually cited because it is considered the most likely of the three SWC ratios (Fig. 1) to be correlated with H_2S-cracking through pipe walls.

Values of %CTR determined on parent and weld SSC specimens, unfailed after immersion at the THS for 720 h, are given in Tables 1 and 2. Our previous investigations suggested that internal crack groups oriented transverse to the applied stress (i.e., with the "t" dimension greater than the "l" dimension in Fig.1) are precursors of cracking failures of SSC specimens (2). A "transverse cracking group" is shown in Fig. 5, and SSC specimens exhibiting one or more of these groups are identified in Tables 1 and 2. These tables also list %CTR values from tests on unstressed SWC coupons, obtained on the mid-thickness metal from which SSC specimen gauge lengths are fabricated. In these coupons, transverse cracking groups were rare.

It is important to recognize that - all else being equal - cracking ratios from SWC coupons will be larger than those from SSC specimens. Compared with the same cylindrical volume in the much larger coupon, the cylindrical gauge length of SSC specimens will show less cracking simply because of the absence of surrounding metal - in which cracks could have initiated, and propagated into the cylinder. A comparison of SWC data obtained on SSC and SWC specimens after an identical test in an H_2S environment is given in Table 5, and confirms that cracking ratios are usually much larger in SWC coupons.

In Fig. 6, %CTR values derived from the SSC and SWC measurements in Table 1 are plotted against YS; the SWC data is represented by a least squares straight line (2). Data from the SSC tests show a strikingly different trend and can be described schematically by a bell-shaped curve with a maximum at lower yield strengths.

Recalling Table 5, SSC specimens showing %CTR values much higher than those for the corresponding SWC coupons would be unexpected, and would indicate that a significant growth of SSC was caused by stressing at the THS

for 720 h. Parent metal SSC specimens from pipes AB, CA, CC and CD showed such SSC growth (Table 1). Transverse crack groups were observed in AB, CA, CB and CD; the presence of these groups will elevate %CTR.

In Fig. 7, the %CTR data of Table 1 are plotted against the ratio THS/YS, which represents intrinsic SSC resistance. It is noteworthy that SSC specimens from the two pipes most resistant to sulphide stress cracking - AG and Z - did not exhibit SWC growth. But SWC growth was also absent in AE and CE, which exhibited only mediocre resistance to SSC.

The data in Table 2 are derived from SSC and SWC tests on specimens containing welds which showed cracking in the HAZ and parent metal, but rarely in the weld fusion zone. The microstructural complexity of weld specimens made experimental results less amenable to analysis, but Fig. 8 shows trends resembling those given for parent specimens in Fig. 7.

Scanning electron microscopy (SEM)

After failure, the fracture surfaces of the SSC specimen were in direct contact with the corrosive H_2S-saturated test solution for 1-60 h. Specimen surfaces were then cleaned by immersion in hydrochloric acid containing a corrosion inhibitor and stored in a dessicator prior to examination by SEM.

Specimens that had failed at the lowest applied stress were considered most likely to show environmentally-induced cracking and were, therefore, selected for fracture surface examination by SEM. The specimens examined and the applied stress/YS ratios causing failure are listed for parent and weld specimens respectively in Tables 6 and 7.

SEM views at low magnification of two fractured parent SSC specimens are given in Fig. 9. As clearly seen in specimen AG-5, fractures generally exhibited areas lying approximately transverse to the specimen axis. These transverse areas were assumed to have been environmentally induced. The more prevalent slanting (shear) surfaces seemed likely to have been formed mechanically after the slower environmental cracking process had weakened the specimen sufficiently for fast fracture to occur. In the SEM examinations at higher magnifications, attempts were made to determine the predominant fracture mechanism(s) on both "transverse" and "shear" planes.

The results of the SEM examinations are summarized in Tables 6 and 7 and indicate that four different fracture mechanisms were observed. Examples

of each of these, as observed in parent metal specimens in areas transverse to the specimen axis, are given in Fig. 10 and 11.

Quasi-cleavage (QC) was the fracture mechanism most frequently observed, and was exhibited by 17/18 specimens on one or both of the two planes examined. Microvoid coalescence (MVC) was shown by 12/18 specimens. This mechanism is often thought to denote mechanical rupture, and in keeping with this, there was a slightly greater proportion of MVC on shear than transverse planes, particularly for parent specimens. But 9/18 specimens showed the same fracture mechanisms on planes identified as "transverse " and "shear". Intergranular attack (IG) was shown by 3/18 specimens while only 2/18 specimens showed comparatively large facets, strikingly different from the features termed QC. These large facets were termed "cleavage" (CL).

Among the parent specimens, AG-5 was from the most SSC-resistant pipe and was the only specimen to show a predominance of MVC over the entire surface. Cleavage, on the other hand, was exhibited only in specimens AE-5 and CC-5, from pipes with mediocre resistance to SSC. CE-5 was unique in showing only IG.

Metallographic sections of the weld specimens confirmed stereomicroscopic observations of the position of the SSC fracture with respect to the WFZ, as listed in Table 7. A relatively deep crack in the WFZ was also detected in specimen AEW-3 (Fig 12). AGW-4 failed in the HAZ, and like the corresponding parent metal SSC specimen, was unique in showing predominant MVC - however, resistance to SSC was only mediocre. ABW-3 and CCW-5 were the most resistant of the weld specimens to SSC, and QC was the predominant mechanism in the transverse plane. But the two weld specimens most susceptible to SSC - AEW-3 and ZW-2 - also showed a predominance of QC on the transverse plane.

In summary, the SEM examinations - considered in isolation from the results of other measurements - were uninformative. There was no obvious correlation of predominant cracking mechanisms to degree of resistance to SSC; nor could areas of environmentally induced cracking be distinguished clearly from those of mechanical fracture.

Some of fracture surfaces showed depressions which apparently had been internal blisters just prior to specimen fracture. An SEM view of such a feature in SSC specimen AB-8 is shown in Fig. 13, and this view also shows the marked delamination in the rolling plane noted in Table 6. Figure 13

also shows a metallographic section of part of the fracture surface of the other half of the same SSC specimen, showing sub-surface blisters in the rolling plane and a relatively large internal blister which has been opened up by the fracture.

Only parent metal from pipe AG showed circumferential cracking on the gauge length surfaces; SSC specimen AG-5 is shown in cross-section in Fig. 14. Cracks are generally blunt and have about the same depth, except for two on the lower surface, deeper and sharper at their tips, that appear to be propagating. One of these is shown at higher magnification in Fig. 14 and exhibits fine intergranular cracking at the tip. The fracture of SSC specimen AG-5 is assumed to have resulted from an intergranular extension of one of the circumferential surface cracks - i.e., by classical SSC.

M. Tanimura has also observed what is referred to in this report as circumferential cracking. He contends that stress-enhanced selective dissolution is producing trenches which are neither cracks nor crack precursors, and that SSC will only initiate in the trenches at applied stresses exceeding THS (3).

EFFECT OF STRESS ON INTERNAL CRACKING

As described above, metallographic examination of SSC specimens, unfailed after 720 h at THS, indicated that these conditions had caused a growth of SWC in some of the pipes. Concurrently with this work, the effect of tensile stress on internal cracking was being examined more systematically in 96 h tests, as reported below.

Location of metal in pipe

Pipes AE, AG, CB and Z were selected for testing, because SWC tests had shown that cracking was concentrated in the centre half-thickness of the pipe wall, from which SSC specimen gauge lengths are made (2,4). It was assumed that a greater susceptibility to SWC would facilitate the study of the effect of stress. Parent metal about 180° around the pipe circumference (P 180) was used, rather than the parent metal about 0° from the weld (P0) of earlier SSC tests. As a preliminary, therefore, the mechanical properties of P 180 metal of the 4 pipes were determined, and standard NACE SSC tests were performed to establish the threshold stress THS.

In Table 8, mechanical properties and SSC resistance parameters of P0 and P 180 SSC specimens of pipes AE, AG, CB and Z are compared. For pipe

Z differences between PO and P 180 mechanical properties were greater than expected. Without a corresponding increase in YS, the intrinsic SSC resistance (as ratio THS/YS) of P 180 metal from pipes AE and CB was distinctly superior to that for PO metal.

The SEM was used to examine fracture surfaces of P 180 specimens failing at the lowest stress - as with the PO specimens listed in Table 6. Predominant fracture mechanism of the PO and P 180 specimens were found to be similar for AE and AG, but rather different for CB and Z, in that cleavage (CL) was seen in the P 180 fracture faces only (Table 9). Evidently, CL is not necessarily found in conjunction with mediocre resistance to SSC, as might have been thought from the results of Table 6 on PO specimens.

Cracking ratios versus tensile stress

To investigate the effect of stress on internal cracking, three replicate SSC specimens of P 180 metal of each of the four pipes selected were stressed at ratios of applied stress/YS of 0, 0.2, 0.4 and 0.6. The stressed specimens were then immersed for 96 h in H_2S-saturated NACE solution.

Internal cracking was evaluated quantitatively in the gauge length of each tested SSC specimen (2,4,5). Values of %CLR/cm^2 and %CTR obtained, and averages at each stress level, are given in Table 10. In no case was a "transverse crack group" (as in Fig. 5) observed. Average values of %CLR/cm^2 and %CTR are plotted against stress level in Fig. 15 and 16.

In view of the typically poor reproducibility shown in Table 10 and the absence of a general trend in Fig. 15 and 16, it is concluded that cracking ratios of AE, AG, CB and Z were essentially unaffected by stresses from 0 to 0.6 YS. This SWC behaviour was for the most part consistent with that shown by the four steels in SSC tests at somewhat higher stresses (Table 1); i.e., none of AE, AG, CB and Z showed SWC growth and only CB showed transverse crack groups.

STEPWISE CRACKING

The NACE has developed standard test method TM-02-84 for evaluating the resistance of pipeline steels to SWC.

STANDARD SWC TESTS

Susceptibility to SWC was evaluated at PMRL using procedures essentially equivalent to test TM-02-84. Details of the procedures used at PMRL have been reported (6).

In brief, rectangular test coupons were prepared, some containing the mill weld, others of parent metal 90° and 180° around the pipe circumference from the mill weld. The unstressed coupons were hydrogen charged by immersion for 4 days in each of two H_2S-saturated solutions - synthetic seawater (B.P. solution) and acidified NaCl (NACE solution).

The tested coupons were then sectioned on a plane normal to the plate rolling direction and examined for SWC. The dimensions of cracks and crack groups were measured and the SWC ratios listed in Fig. 1 calculated. At PMRL, the ratio %CLR/cm^2 or some other normalized function of the %CLR was used after it was realized that the latter is a function of pipe wall thickness T.

EFFECT OF TEMPERATURE ON SWC

Grade 359 pipe CA was chosen for the measurements because it was moderately susceptible to SWC, and exhibited relatively uniform attack around the pipe circumference. A 10 x 10 matrix of parent metal SWC coupons was laid out, centred 180° from the longitudinal weld, with the length of each coupon in the plate rolling direction. The coupons were numbered according to location, and used in the tests in random order.

At temperatures from 0° to 60°C, triplicate coupons of CA were immersed for 4 days in H_2S-saturated NACE solution, after which the hydrogen absorbed by each ca 200 g coupon was measured by displacement of glycerol at 45°C as has been described in detail (7). The absorbed hydrogen was also measured in triplicate on 5 g specimens of CA made from one of the coupons in the matrix. Upon removal from the test solution, the 5 g specimens were immediately immersed in liquid nitrogen prior to having the hydrogen content measured on an automatic analyser (Leybold-Heraeus GMBH) by extraction at 1100°C. In addition, a fourth SWC coupon was tested at each temperature to determine the corrosion rate by mass loss of the descaled coupon.

SWC ratios

%CTR values are given for individual test coupons of CA in Fig. 17, in which the averages at each temperature are shown by a dashed line. Considerable scatter is shown by replicate specimens at each temperature, in agreement with previous experience. The average values of %CTR show a markedly

zig-zag profile suggesting that unidentified deviations in experimental conditions may be causing differences from one test to the next.

The results indicate that temperature has little effect on SWC from 15 to 60°C. At temperatures of 0° and 5°C, %CTR values appear to be higher, indicating more severe conditions.

Plots of %CLR/cm^2 and %CSR vs temperature, not given in this report, show zig-zag profiles in phase with those in Fig. 17, but differ from Fig. 17 in indicating that there is little effect of temperature over the entire range investigated - 0 to 60°C.

Hydrogen analyses

In Fig. 18 the hydrogen absorbed by each coupon, measured as diffusible hydrogen at 45°C, is plotted against temperature*. The zig-zag profile of the average values is to a considerable extent in phase with that in Fig. 17, but there is less scatter shown at each temperature. Increased SWC is indicated at lower temperatures.

A plot of absorbed hydrogen versus %CTR for coupons of CA tested at all temperatures is given in Fig. 19, and confirms earlier work indicating that absorbed hydrogen is related to SWC damage for data obtained on the same steel (4). The dashed line in Fig. 19 is drawn to intersect the horizontal axis at an assumed threshold hydrogen concentration for SWC, C_{th}, of 0.5mL/100 g - considered reasonable for pipe CA on the basis of the findings of Ikeda at al (8).

The hydrogen absorbed during tests, as shown by hot extraction at 1100°C on 5 g specimens of CA, is plotted against temperature in Fig. 20. Scatter at each temperature is much greater than observed in the standard 200 g coupons, probably because of the greater effect of erratic generation of gas-filled internal cracks in small samples.

Comparison of Fig. 20 and 18 indicates similar hydrogen absorption for the two methods for specimens tested above 25°C. Below 25°C, the hot extraction method yields about 2mL/100 g more hydrogen than does collection from glycerol at 45°C.

---

*Because of the failure of silicone oil at 45°C as an alternative to glycerol, results were not obtained for the SWC test at 25°C.

Corrosion rate

The mass-loss corrosion rate at each test temperature, as indicated by a single coupon, is shown in Fig. 21. At temperatures of 30°C or less, the marked zig-zag profile of the corrosion rate data parallels that shown in Fig. 18 by absorbed hydrogen (diffusible at 45°C). It appears, therefore, that reproducibility of experimental conditions could be investigated by means of relatively simple mass-loss corrosion tests.

Figure 21 also shows the percentage of corrosion-produced hydrogen absorbed by test specimens, calculated from both diffusible hydrogen at 45°C and hot extraction. A greater proportion of corrosion hydrogen is shown to be absorbed below 25°C. Above 25°C, the percentage of hydrogen absorbed decreases as corrosion rate increases.

REFERENCES

1. Biefer, G.J. and Fichera, M. "Sulphide stress cracking tests on gas transmission linepipe"; Division Report ERP/PMRL 82-64(TR); CANMET, Energy, Mines and Resources Canada; 1982.

2. Biefer, G.J. and Fichera, M. "Sulphide stress cracking and stepwise cracking tests on gas transmissions linepipes"; Division Report ERP/PMRL 83-17(OP-J); CANMET, Energy, Mines and Resources Canada; 1983. In: Proc of Symp on Effect of Hydrogen Sulphide on Steel at 22nd Ann Conf Metallurg Can Inst Min Metallurg; Aug 22-24, 1983; Edmonton; 1-37; 1983.

3. Tanimura, M. "Private communication to NACE Task Group T-1F-20 - on visual inspection of NACE TM-01-77 test specimen"; Nippon Kokan K.K., Japan, September 1983.

4. Biefer, G.J. and Fichera, M.J. "Evaluation of H_2S-induced stepwise cracking of linepipe"; Division Report ERP/PMRL 83-7(TR); CANMET, Energy, Mines and Resources Canada; 1983.

5. Biefer, G.J. "The stepwise cracking of pipeline steels in sour environments"; Mater Perform 21:6; 19-34; 1982.

6. Fichera, M.J. "Procedure used for stepwise cracking research at PMRL"; Division Report ERP/PMRL 81-51(INT); CANMET, Energy, Mines and Resources Canada; 1981.

7. Selwyn, J.C. "Determination of diffusible hydrogen at 45°C in stepwise cracking measurements on linepipe steel"; Division Report ERP/PMRL 81-58(INT); CANMET, Energy, Mines and Resources Canada; 1981.

8. Ikeda, A., Kaneko, T., Hashimoto, T., Takeyama, M., Sumitomo, Y. and Yamura, T. "Development of hydrogen induced cracking (HIC) resistant steels and HIC test methods for hydrogen sulphide service"; In: Proc of Symp on Effect of Hydrogen Sulphide on Steel, at 22nd Ann Conf Metallurg Can Inst Mining Metallurg; Aug 22-24, 1983; Edmonton; 1-71; 1983.

Table 1 - H_2S cracking resistance parameters of parent SSC specimens unfailed after 720h at threshold stress in H_2S-saturated NACE solution

Spec No.	Yield strength (YS),MPa	SSC threshold (THS),MPA	Ratio THS/YS	Crack thickness ratio, %CTR	
				From tests on stressed SSC specimens (1)	From tests on unstressed SWC coupons (2)
AB-1	518	348	0.672	99 (3)	5.0
AE-4	646	429	0.663	4.9	19
AG-4	597	545	0.912	0	30
CA-5	418	269	0.643	99 (3)	3.1
CB-3	494	336	0.680	68 (3)	69
CC-1	526	317	0.604	28	11
CD-1	416	258	0.620	41 (3)	0.5
CE-1	368	235	0.640	0	0
Z-5	538	459	0.852	1	14

(1) %CTR determined on gauge length after testing parent SSC specimen at THS.

(2) %CTR values are averages, determined on the centre half-thickness of parent metal near the weld, after SWC tests in H_2S-saturated NACE solution.

(3) Section contains crack groups oriented transverse to the stress direction.

Table 2 - H_2S cracking resistance parameters of weld SSC specimens unfailed after 720 h at threshold stress in H_2S-saturated NACE solution.

Spec No.	Yield strength (YS), MPa	SSC threshold (THS), MPA	Ratio THS/YS	Crack thickness ratio, %CTR	
				From tests on stressed SSC specimens (1)	From tests on unstressed SWC coupons(2)
ABW-4	582	410	0.704	14 (3)	21
AEW-4	642	309	0.482	21	12
AGW-5	563	343	0.608	26 (3)	13
CAW-4	432	269	0.623	0	25
CBW-5	510	269	0.528	5.0	14
CCW-4	591	436	0.738	11	20
CDW-1	453	258	0.570	59 (3)	0
CEW-4	374	206	0.550	27	0
ZW-4	614	314	0.511	38	0.9

(1) %CTR determined on gauge length after testing weld SSC specimen at THS.

(2) %CTR values are averages, determined on middle metallographic sections (containing weld, HAZ and some parent metal), after SWC tests in H_2S-saturated NACE solution.

(3) Section contains crack groups oriented transverse to the stress direction.

Table 3 - Types of surface cracking on gauge lengths of parent SSC specimens tested in H_2S-saturated NACE solution

Pipe	Type of cracking*
AB	T>S, B
AE	T, B
AG	C
CA	T, B
CB	T, B
CC	T>S
CD	T>S, B
CE	S>T, B
Z	T

*T = Through-thickness cracking
B = Blistering
S = Side cracking
C = Circumferential cracking
See text and Fig. 3 for definitions

Table 4 - Microstructure in which weld SSC specimens failed, as indicated by stereomicroscopy

Pipe	Microstructure*
AB	HAZ, HAZ
AE	HAZ, HAZ
AG	HAZ, HAZ, WFZ
CA	HAZ, HAZ, HAZ,
CB	HAZ, HAZ, HAZ, P, P
CC	HAZ, HAZ
CD	HAZ, HAZ, P, P
CE	HAZ, HAZ, HAZ
Z	HAZ, HAZ, HAZ

*HAZ = Heat-affected zone of weld
WFZ = Weld fusion zone
P = Parent metal

Table 5 - SWC data obtained in two types of unstressed sample after 4 days in H_2S-saturated NACE solution[1]

Pipe	SSC tensile specimens[2]		Rectangular SWC coupons[3]	
	Av %CTR	Av %CLR/cm^2	Av %CTR	Av %CTR/cm^2
AE	20.5	47.3	22.1	76.5
AG	3.7	9.8	15.3	40.7
CB	14.4	36.1	52.9	93.6
Z	19.2	34.7	43.7	53.0

(1) In both cases, parent metal 180° from the weld was used

(2) These SSC specimens did not exhibit any transverse crack groups

(3) SWC ratios obtained in the centre half-thickness of the pipe wall

Table 6 - SEM examination of fracture surface of parent SSC specimens

Spec No.	SSC test ratio: Applied stress / Yield stress	Fracture mechanisms* Transverse plane	Shear plane	Notes
AB-8	0.708	QC	MVC	Marked delamination on rolling plane.
AE-5	0.700	QC>CL	QC>CL	AE-5,CC-5 similar in appearance.
AG-5	0.946	MVC>QC	MVC	-
CA-3	0.686	QC>MVC	QC>MVC	Marked delamination on rolling plane.
CB-4	0.705	QC	MVC	Marked delamination on rolling plane.
CC-5	0.642	QC>CL	QC>CL	AE-5,CC-5 similar in appearance.
CD-5	0.658	QC>MVC	QC	-
CE-5	0.680	IG	IG>QC	-
Z-4	0.897	QC>MVC	MVC	-

*QC = Quasi-cleavage
MVC = Microvoid coalescence
CL = Cleavage
IG = Intergranular

Table 7 - SEM examination of fracture surface of weld SSC specimens

Spec No.	SSC test Ratio: Applied stress / Yield stress	Fracture mechanisms*		Notes**
		Transverse plane	Shear plane	
ABW-3	0.746	QC	MVC	Fracture in HAZ.
AEW-3	0.519	QC	QC	Fracture in HAZ. Isolated crack in WFZ.
AGW-4	0.645	MVC>QC	MVC>QC	Fracture in HAZ.
CAW-1	0.664	QC,MVC	QC, MVC	Fracture mostly in HAZ; also in parent metal.
CBW-6	0.548	QC>MVC	MVC	Fracture in parent metal.
CCW-5	0.772	QC>MVC	QC>MVC	Fracture in HAZ.
CDW-5	0.605	QC>IG	QC>IG	Fracture mostly in parent metal; also in HAZ.
CEW-5	0.590	IG	IG	Fracture in HAZ
ZW-2	0.511	QC>MVC	MVC>QC	Fracture in HAZ.

*QC = Quasi-cleavage.
MVC = Microvoid coalescence.
CL = Cleavage.
IG = Intergranular
**Based on both SEM and examination of metallographic sections through the fractures.

Table 8 - Mechanical properties and SSC resistance parameters for parent metal SSC specimens from two different locations in the pipes*

Pipe	Location of SSC specimen in parent metal	Mechanical properties			SSC parameters	
		YS, MPa	UTS, MPa	Elong, %	THS, MPa	Ratio, THS/YS
AE	PO	646	744	21.5	429	0.664
	P180	640	762	21	524	0.819
AG	PO	597	678	25	545	0.913
	P180	578	668	25.5	543	0.939
CB	PO	494	600	28.5	336	0.680
	P180	519	634	23.5	456	0.879
Z	PO	538	673	26	459	0.853
	P180	486	609	32	376	0.774

*YS = Yield strength.
UTS = Ultimate tensile strength.
THS = Threshold stress for resistance to SSC.
PO = Parent metal about 0° from weld.
P180 = Parent metal about 180° from weld.

Table 9 - SEM examination of fracture surface of parent metal specimens from two different locations in pipes

Pipe No.	Location* of specimen	Fracture mechanisms**	
		Transverse plane	Shear plane
AE	PO	QC>CL	QC>CL
	P180	QC>CL	QC>CL
AG	PO	MVC>QC	MVC
	P180	MVC>QC	MVC
CB	PO	QC	MVC
	P180	QC>MVC,CL	QC>MVC,CL
Z	PO	QC>MVC	MVC
	P180	QC>CL	MVC,QC>CL

*PO = Parent metal,0° from weld.
P180 = Parent metal, 180° from weld.
**QC = Quasi cleavage.
MVC = Microvoid coalescence.
CL = Cleavage.

Table 10 - Effect of tensile stress on internal cracking (as SWC ratios) in SSC specimens immersed 4 days in H_2S-saturated NACE solution.

Pipe	Ratio: Applied stress / YS	AV % CTR	AV % CLR/cm^2
AE	0	20.5 (22.6, 16.0, 22.9)	47.3 (47.5, 45.7, 48.6)
	0.2	27.6 (29.0, 27.1, 26.7)	56.3 (61.4, 51.8, 55.8)
	0.4	22.9 (20.8, 15.1, 32.7)	44.6 (47.1, 29.9, 56.9)
	0.6	27.9 (24.1, 39.8, 19.8)	48.3 (45.7, 70.2, 29.1)
AG	0	3.7 (0.9, 4.6, 5.5)	9.8 (1.4, 12.4, 15.5)
	0.2	6.1 (2.7, 8.2, 7.4)	12.0 (8.6, 15.8, 11.5)
	0.4	12.8 (15.5, 11.8, 11.1)	16.7 (19.3, 17.0, 13.9)
	0.6	9.8 (6.4, 14.8, 8.3)	12.5 (10.2, 12.8, 14.6)
CB	0	14.4 (9.6, 15.4, 18.3)	36.1 (43.9, 31.9, 32.6)
	0.2	9.0 (4.6, 8.3, 14.0)	12.7 (15.8, 13.3, 9.1)
	0.4	4.9 (5.5, 3.7, 5.5)	17.1 (20.3, 20.7, 10.3)
	0.6	22.7 (24.3, 18.9, 25.0)	22.9 (12.3, 20.3, 36.0)
Z	0	19.2 (14.7, 30.7, 12.3)	34.7 (26.0, 50.4, 27.6)
	0.2	20.2 (21.9, 19.8, 18.9)	23.7 (21.5, 27.3, 22.2)
	0.4	17.3 (17.0, 17.8, 17.1)	22.9 (26.7, 20.2, 21.8)
	0.6	17.3 (19.8, 19.6, 12.4)	25.2 (18.0, 31.1, 26.5)

A1.

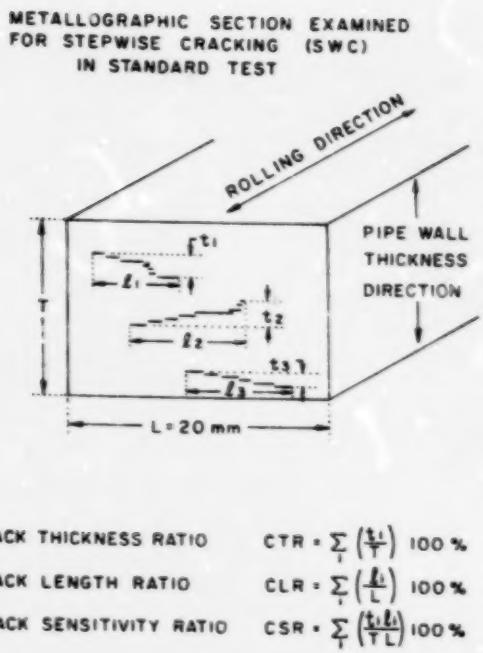
METALLOGRAPHIC SECTION EXAMINED
FOR STEPWISE CRACKING (SWC)
IN STANDARD TEST
ROLLING DIRECTION
PIPE WALL
THICKNESS
DIRECTION
T
L = 20 mm
CRACK THICKNESS RATIO CTR = $\sum_i \left(\frac{t_i}{T}\right)$ 100 %
CRACK LENGTH RATIO CLR = $\sum_i \left(\frac{\ell_i}{L}\right)$ 100 %
CRACK SENSITIVITY RATIO CSR = $\sum_i \left(\frac{t_i \ell_i}{T L}\right)$ 100 %

Fig. 1. Metallographic plane examined in standard SWC coupons and in the gauge length of SSC specimens. In SSC tests, stress is applied in a direction parallel to the L dimension. (neg 7831)

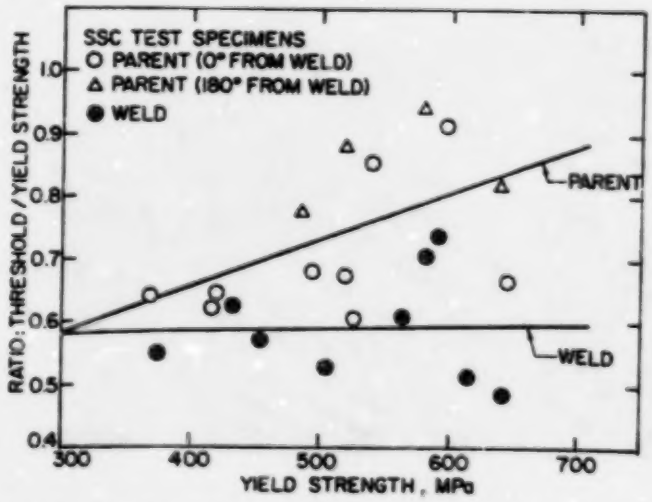

Fig. 2. Least squares plots of data from SSC tests in H_2S-saturated NACE solution on parent and weld specimens of gas transmission pipes. (neg 10114)

A1.

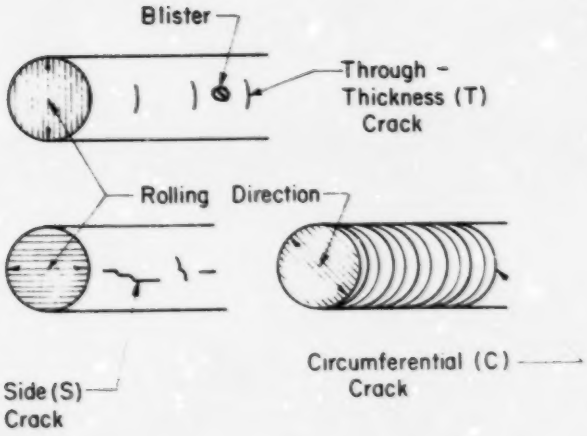

SCHEMATIC DIAGRAM OF TYPES OF SURFACE CRACKING IN SSC TESTS

Fig. 3. Different types of surface cracking observed on gauge lengths of SSC specimens after testing in H_2S-saturated NACE solution. (neg 9423)

Fig. 4. SEM view of circumferential (C) cracking in parent SSC specimen AG-5. Specimen axis is vertical on the page. (neg 9275)

A1.

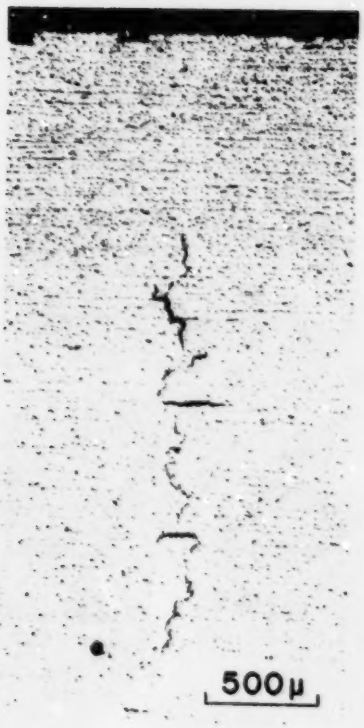

Fig. 5. Transverse crack grouping in parent metal SSC specimen from pipe CB, u[illegible]ailed after testing at the THS for 720 h. The plane of the metallographic section is normal to the plate rolling direction and the direction of the applied tensile stress is horizontal on the page. (neg 8040)

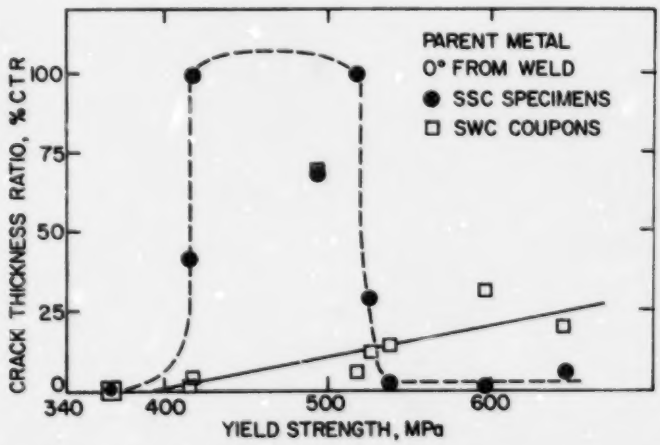

Fig. 6. %CTR values determined on (i) unfailed parent metal SSC specimens after 720 h at the threshold stress THS and on (ii) unstressed SWC coupons - both plotted against SSC specimen yield strength. (neg 10120)

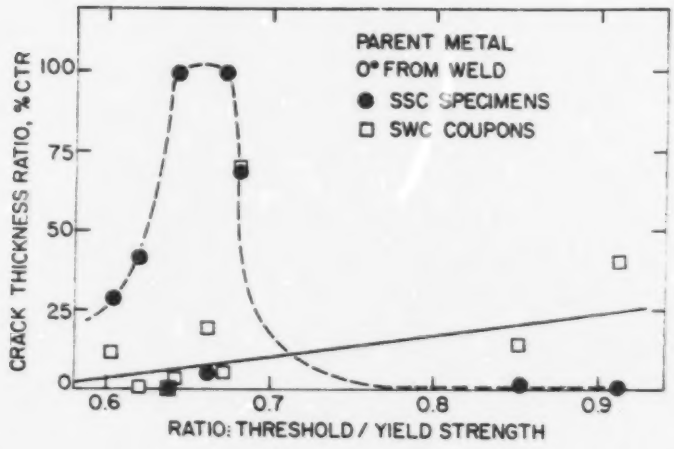

Fig. 7. %CTR values determined on (i) unfailed parent metal SSC specimens after 720 h at the threshold stress THS and on (ii) unstressed SWC coupons - both plotted against the ratio threshold stress/yield strength. (neg 10122)

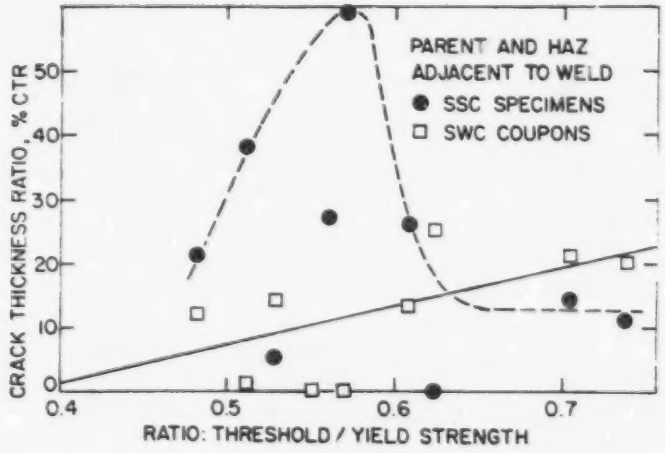

Fig. 8. %CTR values determined on (i) unfailed weld SSC specimens after 720 h at the threshold stress THS and on (ii) unstressed SWC weld coupons - both plotted against the ratio threshold stress/yield strength. (neg 10124)

A1.

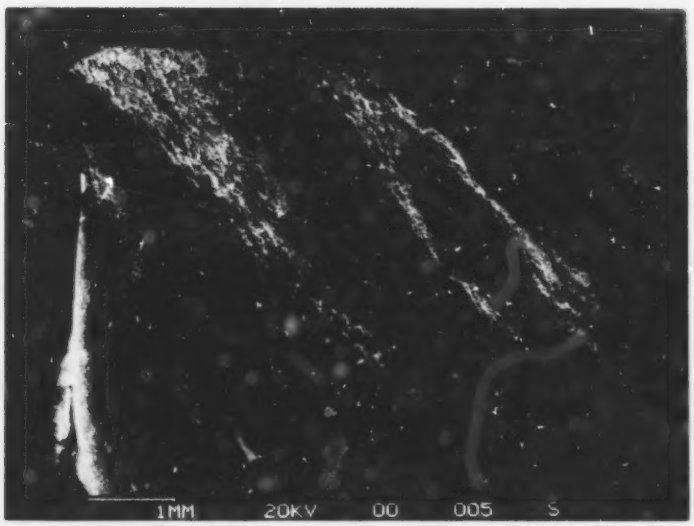

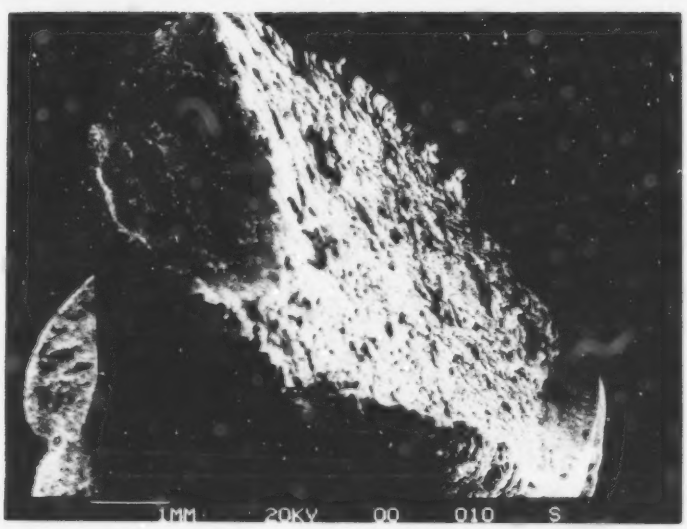

Fig. 9. SEM views of fracture surfaces of AE-5 (upper) and AG-5 (lower) parent SSC sepcimens at low magnification. (negs 10040 and 10041)

A1.

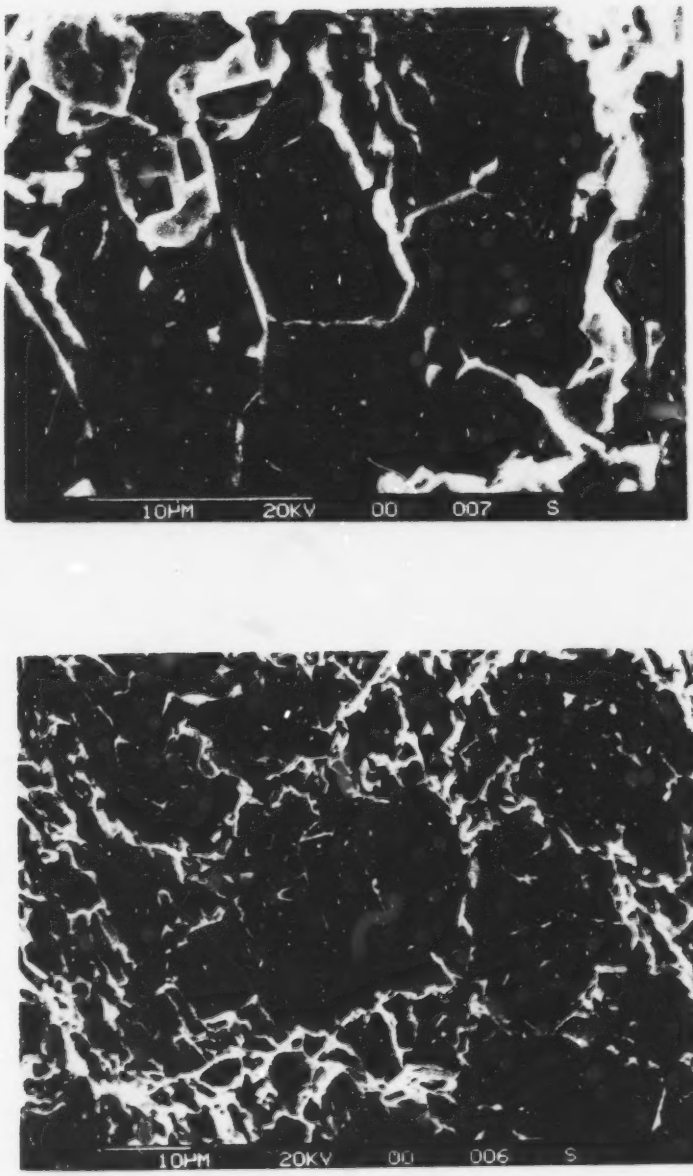

Fig. 10. SEM views of fracture surfaces transverse to specimen axis in parent SSC specimen AE-5 showing cleavage (upper) and cleavage surrounded by quasi-cleavage (lower). (negs 10042 and 10043)

A1.

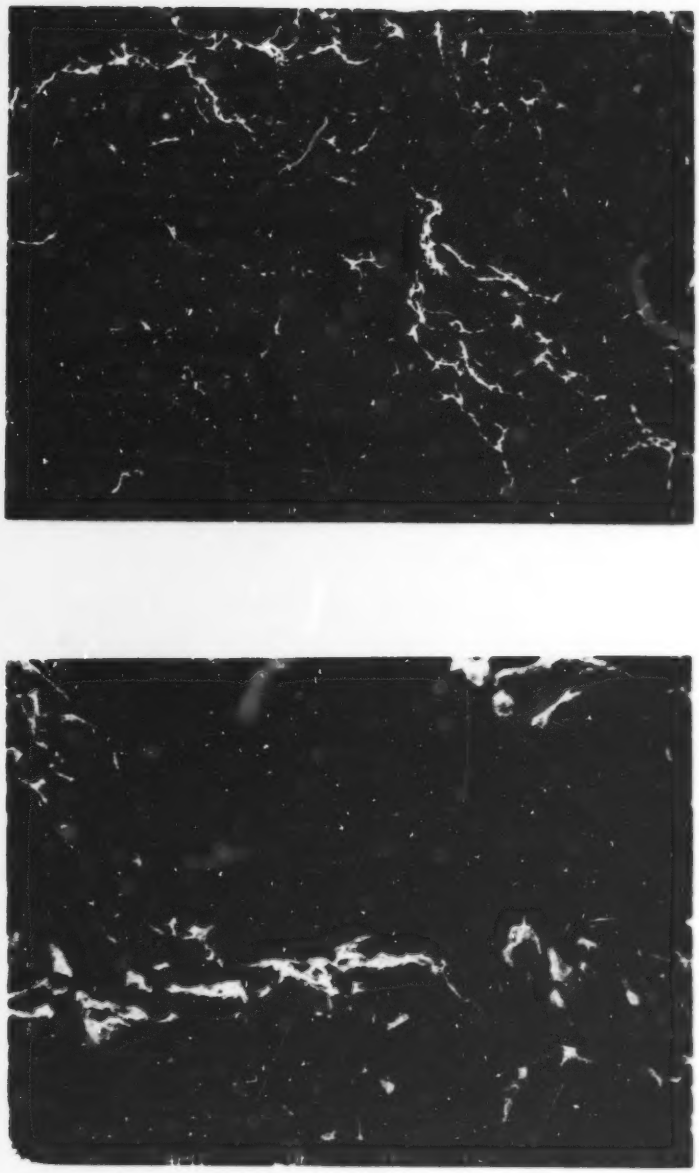

Fig. 11. SEM views of fracture surfaces transverse to specimen axis in parent SSC specimen AG-5 showing microvoid coalescence (upper) and specimen CE-5 showing intergranular attack (lower). (negs 10039 and 10044)

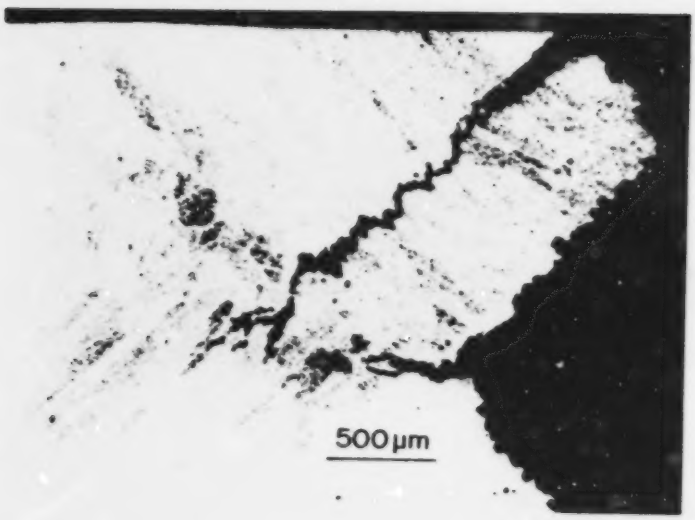

Fig. 12. Metallographic section showing weld fusion zone crack in SSC specimen AEW-3. Fracture surface is at right. (neg 10579)

A1.

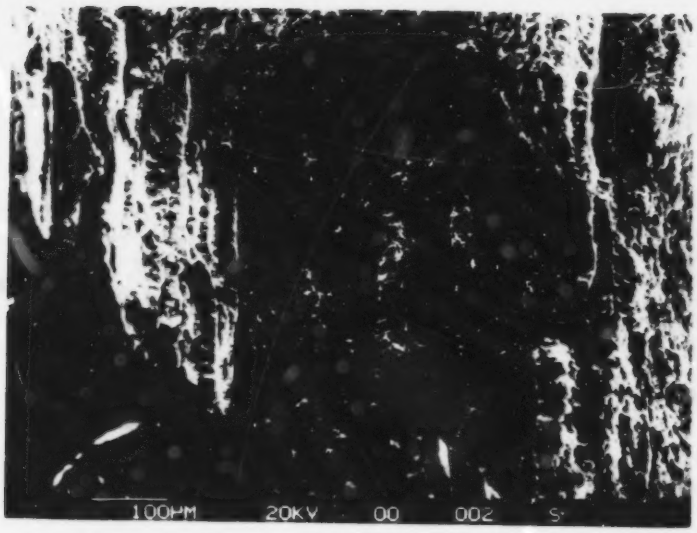

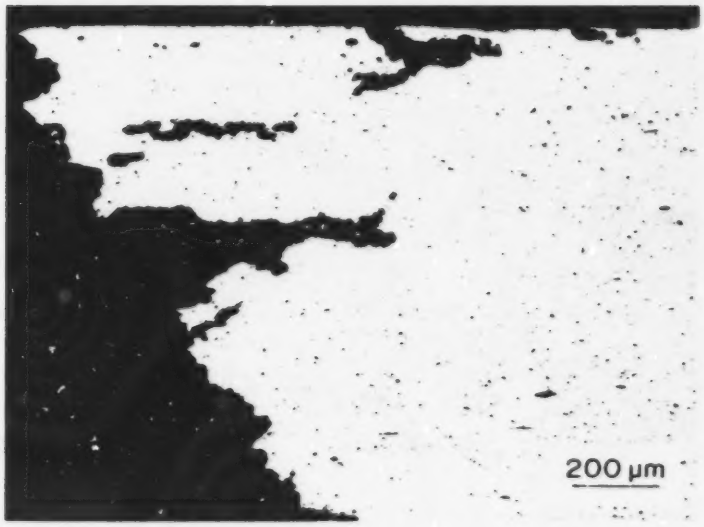

Fig. 13. SEM view of apparent prior blister on fracture surface of SSC specimen AB-8 (upper); and metallographic section of the other half of this fracture surface, showing internal blisters (lower). Fracture surface is at left of lower photograph. (neg 10038 and 10578)

A1.

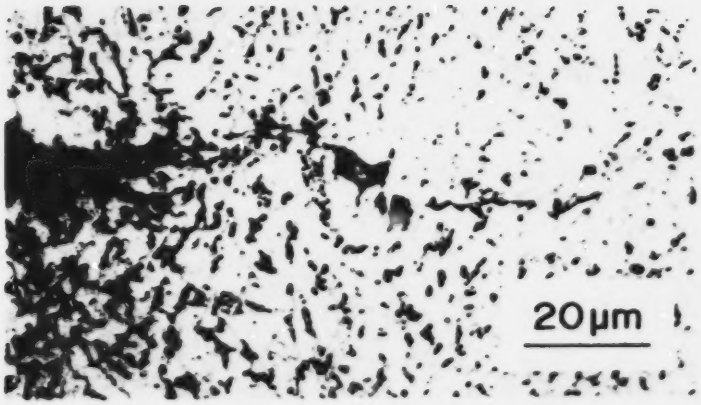

Fig. 14. Metallographic sections showing circumferential cracking in SSC specimen AG-5: (i) entire fracture face and part of gauge length (upper); (ii) intergranular propagation at tip of crack (lower). (negs 10575 and 10576)

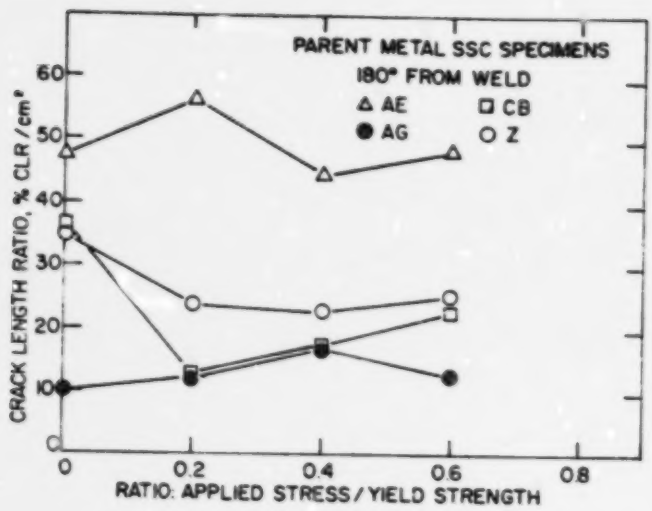

Fig. 15. Av %CLR/cm^2 versus ratio: Applied stress/YS. Tests were run in triplicate on parent metal (180° from weld) SSC specimens in H_2S-saturated NACE solution. (neg 10117)

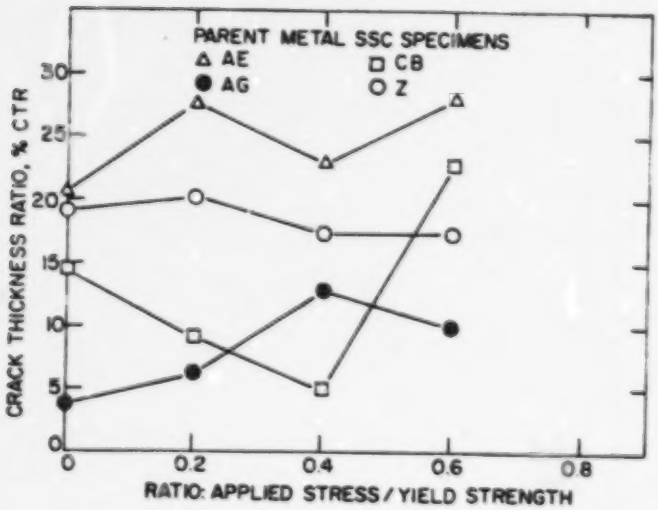

Fig. 16. Av %CTR versus ratio: Applied stress/YS. Tests were run in triplicate on parent metal (180° from weld) SSC specimens in H_2S-saturated NACE solution. (neg 10121)

A1.

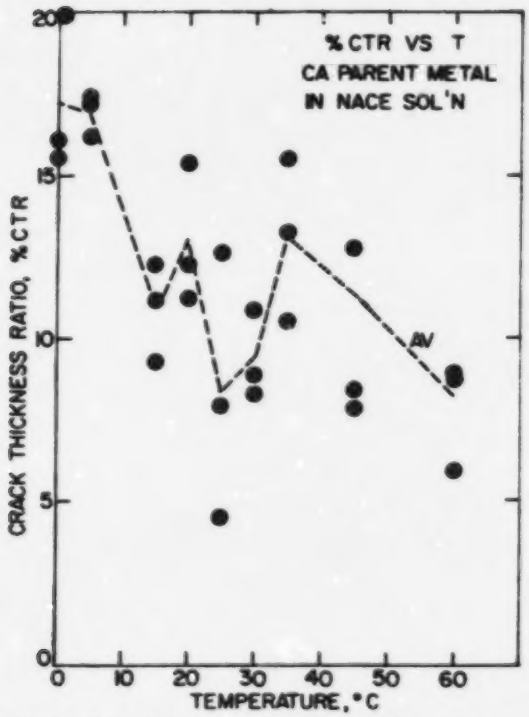

Fig. 17. %CTR versus temperature for SWC coupons of parent metal CA tested in H_2S-saturated NACE Solution. The average value at each temperature is shown by the dashed line.(neg10119

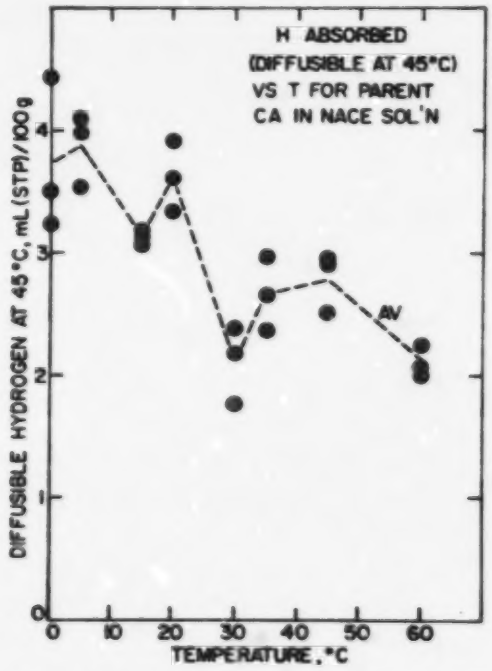

Fig. 18. Hydrogen absorbed (diffusible at 45°C) versus temperature for SWC coupons of parent metal CA tested in H_2S-saturated NACE solution. The average value at each temperature is shown by the dashed line. (neg 10118)

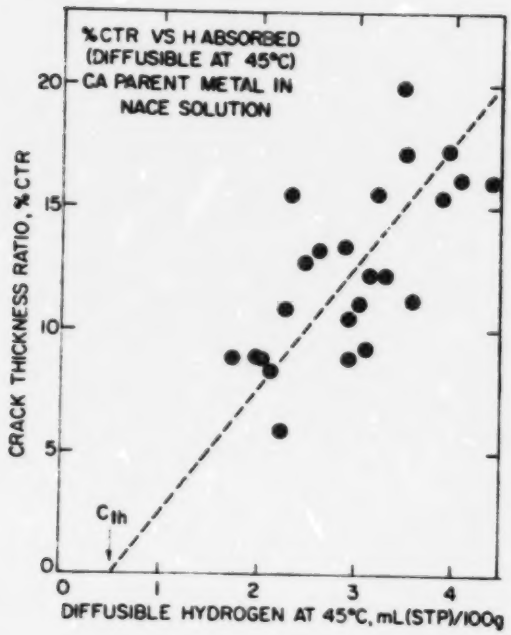

Fig. 19. %CTR vs absorbed hydrogen (diffusible at 45°C) for SWC coupons of CA parent metal tested in H_2S-saturated NACE solution at temperatures from 0 to 50°C. The dashed line is schematic, and drawn to intersect the horizontal axis at an assumed C_{th} value of 0.5 mL/100 g. (neg 10123)

A1.

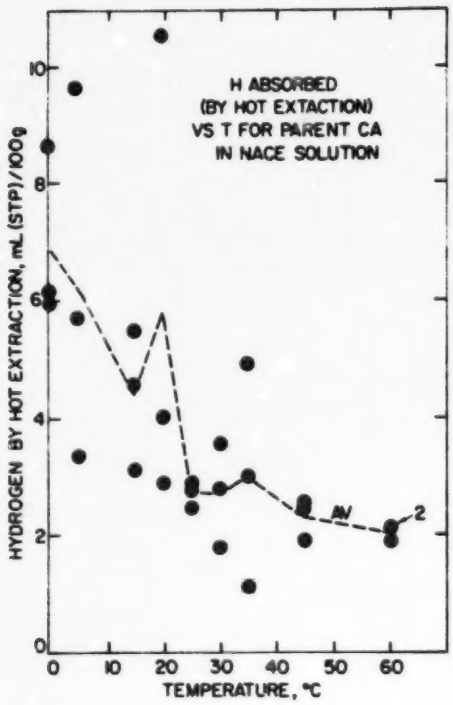

Fig. 20. Hydrogen absorbed (by hot extraction) vs temperature for 5-g specimens of parent metal CA tested in H_2S-saturated NACE solution. The average value at each temperature is shown by the dashed line.
(neg 10125)

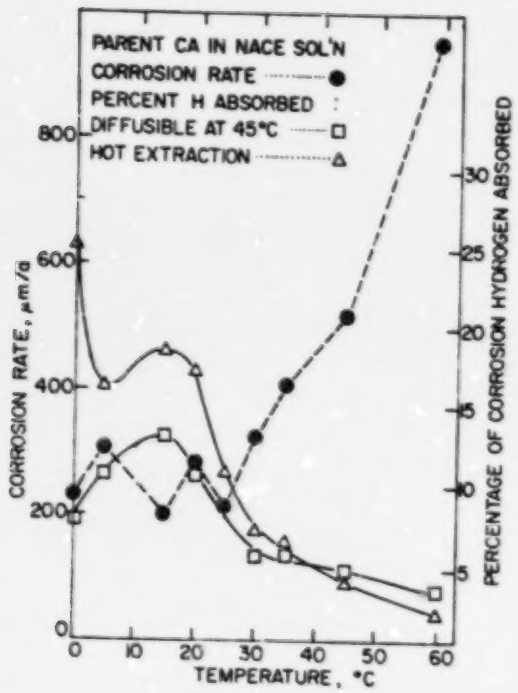

Fig. 21. Corrosion rate versus temperature for SWC coupons of parent metal CA tested in H_2S-saturated NACE solution, showing percentage of corrosion hydrogen absorbed according to two methods of measurement. (neg 10126)

APPENDIX 2

EFFECTS OF NON-METALLIC INCLUSIONS ON STEPWISE CRACKING BEHAVIOR OF LINE-PIPE STEELS

by

M.T. Shehata, G.J. Biefer and J.D. Boyd

Physical Metallurgy Research Laboratories

CANMET

Ottawa, Canada

ABSTRACT

A quantitative metallographic analysis of non-metallic inclusions, and stepwise cracking (SWC) tests in a wet H_2S environment have been carried out for nine commercial line-pipe steels. A Quantimet 900 image analyser was employed for the quantitative metallography, and SWC susceptibility was characterized by the standard NACE (BP) test. An image analysis technique was developed which produces a measurement of inclusions that correlates well with SWC behaviour. This technique demonstrates the importance of elongated sulphide-stringers and planar groups of other inclusion phases in the SWC process. There were some deviations from this correlation. Semi-killed steels exhibited a lower incidence of SWC than that predicted by inclusion measurements, and a fully-killed steel with a heavily banded microstructure had a higher incidence of SWC.

INTRODUCTION

There are several distinct hydrogen-related cracking mechanisms in line-pipe steels. Stepwise cracking is the phenomenon whereby hydrogen accumulates at internal microvoids which have previously formed at the interfaces of non-metallic inclusions, and crack extension results from the internal pressure of the accumulated molecular hydrogen. Due to the aligned nature of the microstructure in controlled rolled line-pipe steels, the cracks appear as groups of thin crack segments parallel to the rolling plane. Nearby cracks can link up, and a macrocrack can propagate in a stepwise manner through the wall of the line pipe. An example of such a crack is shown in Fig. 1. This phenomenon has been studied extensively, and it is variously referred to as stepwise cracking (SWC), hydrogen induced cracking (HIC), hydrogen blister cracking, and hydrogen induced stepwise cracking[1-10].

SWC is a problem for those line-pipe steels that have a yield strength $\leq$ 552 MPa (80 ksi) when they are exposed to a wet H_2S environment. Under these conditions, a corrosion reaction occurs at the surface and atomic hydrogen is produced, which diffuses into the steel and accumulates as molecular hydrogen at inclusion/microvoid sites. In practice, the susceptibility to SWC in line-pipe steel is reduced by alloy additions (eg. Cu, W, Cr or Ni) which inhibit the formation and/or absorption of atomic hydrogen at the steel surface; by reducing the volume fraction and size of non-metallic inclusions (eg. calcium injection, vacuum degassing); and by generally increasing the through-thickness toughness of the steel (eg. segregation control, inclusion control, low C, P, Mn, uniform microstructure)[2].

The metallurgical aspects of SWC centre on the formation of internal blister cracks by the accumulation of hydrogen at inclusion microvoids, the extension of these cracks parallel to the rolling plane by the internal hydrogen pressure, and the linking of nearby cracks along directions inclined to the rolling plane by plastic deformation and fracture. The formation of blister cracks seems to be directly related to the type and distribution of non-metallic inclusions in the steel. Elongated type II MnS inclusions and planar arrays of oxides or complex oxy-sulphide inclusions are preferential sites for blister crack initiation[1,3]. Extension of blister cracks takes

place along paths of low fracture resistance parallel to the rolling plane. The exact nature of these fracture paths is not known. It has been suggested that they are bands of certain transformation products in the steel (eg. martensite or bainite)[4], inclusion/matrix interfaces[5], possibly aided by segregation of C or P[2,3], textured ferrite[5], or some combination of the above. The linking of nearby cracks takes place along bands of localized shear which result from the internal hydrogen pressure acting on elongated blister cracks. The maximum shear stress occurs at the tip of such cracks, and fracture in the shear bands is predominantly by ductile rupture, although rolling-plane blister cracks are also observed[6]. The SWC process can be affected to a certain extent by the application of an external stress. For line pipe the principal external stress would normally be the hoop stress in the pipe due to the gas or oil pressure, and would act in the rolling plane transverse to the rolling direction. Note, however, that the basic process of SWC does not change with the application of an external stress, and is quite distinct from the process of sulphide stress cracking (SSC), which requires an external tensile stress and occurs only in steels having yield strengths $\geq$ 621 MPa (90 ksi).

The objective of the present work was to investigate in detail the relationship between non-metallic inclusions and SWC behaviour in line-pipe steels. Extensive quantitative measurements of several inclusion parameters were made using automatic image analysis equipment, and were correlated with the results of standard SWC tests. This work was part of a comprehensive study of SSC and SWC behaviour of commercial line-pipe steels which will be reported later.

EXPERIMENTAL PROCEDURE AND RESULTS

MATERIALS

Nine commercial line-pipe steels were studied. The designation used for each steel, the pipe grade and details of the processing are given in Table 1. The manufacturers'chemical analyses are given in Table 2.

SWC Tests

SWC tests were carried out according to NACE standard TM-02-84[11]. Three test coupons were cut from each pipe approximately opposite the mill

weld. The specimens were 100 mm long (plate rolling direction), 20 mm wide (transverse direction), and T mm thick, where T was the pipe wall thickness less a small machining loss (T was approximately 12 mm for all steels except CD for which T ≈ 8 mm). After dry grinding and degreasing, the coupons were immersed for 96 h in an H_2S-saturated "B.P. solution" (ASTM D-1141), with initial pH = 5.5. The ratio of solution volume to specimen area was approximately 9 mL/cm^2.

After exposure, 3 metallographic sections were cut from each coupon, normal to the plate rolling direction. Metallographic specimens were prepared by standard procedure and examined by optical microscopy. Three quantities were measured to evaluate SWC for each test coupon, as illustrated in Fig. 2:

1) crack sensitivity ratio (CSR), which is the total area of individual groups of blister cracks per unit area of test coupon,
2) crack length ratio (CLR), which is the total length of individual groups of blister cracks per unit width of test coupon (reported as length/area to compensate for variable thickness of test coupons),
3) crack thickness ratio (CTR), which is the total width of groups of blister cracks per unit thickness of test coupon.

The results of these measurements are given in Table 3. The error reported for each measurement is the standard error of the mean calculated from the variation in the results for 9 sections (3 sections from each of 3 test coupons for each steel).

Quantitative Metallography

Metallographic specimens were prepared of sections perpendicular to the rolling direction for all the steels, and were examined in the as-polished condition by optical microscopy. Several types of non-metallic inclusions were observed. Steels AB, CA and CD contained elongated manganese sulphides, which were often in the form of broken stringers. Highly elongated silicate inclusions were also present in steels AB and CD. The other steels (AE, AG, CB, CC, CE and Z) contained mostly ellipsoidal sulphide inclusions, which had been only slightly deformed by rolling. Some of these inclusions were enclosed by or attached to small oxide particles. Most steels contained a dispersion of angular inclusions which were either alumina or calcium aluminate. In many cases the ellipsoidal or angular inclusions occurred as planar arrays of particles.

Quantitative measurements of inclusion distributions were obtained using a "Quantimet 900" image analysing computer. Approximately 30 fields were measured on each metallographic sample, which corresponded to a total area of 120 mm^2. In order to obtain measurements of inclusions which could be directly compared to the SWC measurements, the optical images of inclusions were automatically amended to account for broken stringers, planar arrays of angular or ellipsoidal particles, and adjacent stringers (Fig. 3). The procedure was as follows:

1) All inclusions were measured together i.e., no distinction was made between sulphides, oxides, silicates, etc.
2) By the technique of directional dilation and erosion, particles spaced $\leq$ 100 µm in the transverse direction (w.r.t. plate rolling) and $\leq$ 25 µm in the through-thickness direction were joined and measured as one particle, (eg. Fig. 3a,b,c). When adjacent particles were outside these dilation distances, the image was not affected, (eg. Fig. 3d).
3) All inclusions $\leq$ 20 µm in length (after image amending) were rejected and were not measured.

With this image analysis procedure, the only inclusions measured were elongated stringers, angular or ellipsoidal inclusions in planar groupings, and discrete particles $\geq$ 20 µm in length. For such images, the total length in the transverse direction per unit area and the area fraction were measured. The results are given in Table 4. The error reported for each measurement is the standard error of the mean calculated from the variation in the results for 30 fields.

In Fig. 4, the total length of blister cracks per unit area (CLR) is plotted against the total length (in the transverse direction) of amended inclusion images per unit area, and in Fig. 5 the area per cent of blister cracks (CSR) is plotted against the area per cent of amended inclusion images. Both plots show a good correlation between the SWC behaviour and the inclusion measurements, with the exception of steels AB, CD and AE. Since the CLR and the total length of amended inclusion images have a more obvious relation as the SWC mechanism, only the correlation between these 2 quantities is discussed below.

DISCUSSION

This work demonstrates that the CLR parameter determined in the standard NACE SWC test correlates well with the total length of amended inclusion images (in the transverse direction) per unit area. Clearly, the effectiveness of this correlation depends on the image-amendment procedure which is used. The procedure used in this study was designed to produce amended images of groups of inclusions which corresponded closely to the observed blister cracks. It emphasized the importance of elongated inclusions and planar groups of angular or ellipsoidal inclusions. Note that the CLR is numerically only about 1/20 of the total length of amended inclusion images per unit area (Fig. 4). This may seem to suggest that only a small fraction of the inclusions are associated with blister cracks, but it is also a consequence of the image amending procedure. By joining separated inclusions which are within the defined dilation distances, the effective inclusion length is increased. However, even when this bias is considered, the CLR remains less than the measured inclusion length. Furthermore, if the minimum length of measured inclusion is increased from 20 μm to 200 μm, the degree of correlation between CLR and the total length of amended inclusion images per unit area does not change significantly, but the ratio of these 2 quantities increases to about 1/7. This indicates that the very long inclusions or large planar groups of inclusions are primarily responsible for SWC, and that for the exposure time used only a minor fraction of all such inclusions are associated with the measured blister cracks.

Of the 3 steels which exhibited anomalous results, AB and CD showed much less cracking than that predicted by the correlation with inclusion measurements, and steel AE showed much more. Steels AB and CD are the only semi-killed steels, and their behaviour is consistent with the general observation that semi-killed steels are less susceptible to SWC than fully-killed steels[1]. The elongated inclusions in steels AB and CD are predominantly silicates which are more plastic than the type II MnS at rolling temperatures. This should result in fewer microvoids at inclusion/matrix interfaces in the semi-killed steels. In addition, steel AB contained 0.22 pct. Cu, which generally reduces susceptibility to SWC.

The most likely explanation for the anomalously high incidence of cracking in steel AE is its heavily banded microstructure compared with the other steels (Fig. 6). It has been proposed that heavily banded microstructures provide paths of low fracture resistance for extending blister cracks, either through low temperature transformation products[4] or textured ferrite[5]. This effect is illustrated by comparing the SWC results for steels AE and AG. The two steels have similar inclusion measurements, but the CLR for AE is much higher than for AG, which has a uniform microstructure. In a separate study, it was also shown that steel AE has much lower fracture toughness under a through-thickness stress, and much higher incidence of rolling-plane delaminations than steel AG[12].

The anomalous results illustrate the effects of factors other than in addition to inclusions in SWC behaviour and emphasize that the correlation with inclusion measurements is valid only when the other factors remain constant.

To summarize, an image analysis technique has been developed to produce a measurements of inclusions which correlates well with SWC behaviour for most fully-killed steels. This technique emphasizes the importance of elongated sulphide stringers and planar groups of other inclusion phases in SWC, which agrees with the observations of other workers[1-10]. Further work is required to determine how the critical inclusion parameter (i.e. the total length of amended inclusion images per unit area) is controlled by the composition and processing of the steel.

CONCLUSIONS

1) The present metallographic study showed that for fully-killed steel the SWC formed during exposure to H_2S-saturated synthetic sea water can be correlated with elongated sulphide inclusions and planar groups of other inclusions present in the steel.
2) In addition to non-metallic inclusions, the microstructure may also play a role in SWC. In particular, heavily banded microstructures could enhance SWC by providing low fracture resistance paths along which cracks propagate more easily.

3) It appears that semi-killed steels have higher resistance to SWC than fully-killed steels.

ACKNOWLEDGEMENTS

The authors express their appreciation to B.R. Casault and M.J. Fichera for technical assistance.

REFERENCES

1. G.J. Biefer, "The stepwise cracking of line-pipe steels in sour environments" Materials Performance, Vol. 21, No. 6, pp. 19-34 (1982).

2. "Corrosion of line-pipe steels in CO_2-H_2S-brine system (sour environment)", Nippon Steel Corp. report, March, 1980.

3. G.M. Pressouyre et al "Very low inclusion and impurity content steels as a solution to resist sour environments". Proceedings of the First International Conference "Current Solutions to Hydrogen Problems in Steels", American Society for Metals, Metals Park OH, pp. 212-218 (1982).

4. A. Ikeda et al, "Hydrogen induced cracking (HIC) susceptibility of various steel line-pipes in the wet H_2S environment", NACE National Conference, 1978, Houston, Paper No. 43.

5. A.P. Coldren and G. Tither, "Metallographic study of hydrogen-induced cracking in line-pipe steels" J. Metals, Vol. 28 No. 5 pp. 5-10 (1976).

6. M.Iino, "The extension of hydrogen blister-crack array in line-pipe steels". Metallurgical Transactions, Vol. 9A, pp. 1581-1590 (1978).

7. T. Murata et al, "Hydrogen-induced cracking in steels and its causes", Tetsu-Tu-Hagane, Vol. 61, S-235 (1975).

8. M. Tanimura and T. Nishimura, "Relationship between susceptibility to hydrogen-induced cracking and properties in short transverse direction of steel plates", Tetsu-Tu-Hagane, Vol. 61, S-241 (1975).

9. H. Nakasugi et al, "Development of new linepipe steels for sour-gas service" Nippon Steel Technical Report No. 14, pp. 66-78 (1979).

10. S.W. Ciaraldi, "Microstructural observations on the sulfide stress cracking of low alloy steel tubulars", Corrosion, Vol. 40, No. 2, pp. 77-81 (1984).

11. National Association of Corrosion Engineers; "Test Method: evaluation of pipeline steels for resistance to stepwise cracking", NACE Standard TM-02-84' Houston, U.S.A. (1984).

12. J.D. Boyd et al, "Fracture modes and microstructure in linepipe steels", unpublished work. Private conversation PMRL 568 Booth Street. Ottawa, K1A 0G1.

Table 1 - Description of commercial line-pipe steels.

Code	Grade	Deoxidation	Casting	Plate Rolling
AB	483 (X70)	Si (semi-killed)	ingot cast	controlled rolled
AE	483 (X70)	Si + Al (fully-killed)	ingot cast	controlled rolled
AG	483 (X70)	Si + Al (fully-killed)	ingot cast	controlled rolled
CA	359 (X52)	Si + Al (fully-killed)	ingot cast	controlled rolled
CB	448 (X65)	Si + Al (fully-killed)	ingot cast	controlled rolled
CC	483 (X70)	Si + Al (fully-killed)	ingot cast	controlled rolled
CD	290 (X42)	Si (semi-killed)	ingot cast	hot rolled
CE	359 (X52)	Si + Al (fully-killed)	continuous cast	controlled rolled
Z	483 (X70)	Si + Al (fully-killed)	ingot cast	controlled rolled

Table 2 - Manufacturers' chemical analyses of steels (wt. pct.).

Element	AB	AE	AG	CA	CB	CC	CD	CE	Z
C	0.06	0.08	0.08	0.13	0.12	0.060	0.22	0.068	0.049
Mn	1.80	1.98	1.70	1.17	1.48	1.76	0.85	0.86	1.94
P	0.009	0.011	0.014	0.005	0.011	0.004	0.004	0.006	0.007
S	0.017	0.005	0.004	0.016	0.010	0.006	0.028	0.001	0.011
Si	0.02	0.29	0.15	0.27	0.27	0.25	0.06	0.256	0.28
Nb	0.058	0.045	0.072	0.015	0.038	-	-	0.020	0.060
Sn	0.02	0.005	0.015	-	0.002	-	-	-	-
Cu	0.22	0.053	0.23	-	0.029	0.028	-	-	-
Ni	0.11	0.033	0.20	-	0.012	0.009	-	0.37	-
Cr	0.04	0.097	0.09	-	0.057	0.044	-	-	-
Mo	0.27	0.24	0.21	-	0.007	0.212	-	-	0.489
V	-	0.05	-	-	0.040	0.035	-	-	-
Al	-	0.017(1)	-	-	0.024(1)	0.034(1)		0.024(2)	
Ca	-	-	-	-	-	-	-	0.0037	-

(1) Acid-soluble Al

(2) Total Al

Table 3 - Results of SWC tests in H_2S-saturated synthetic sea water (B.P. test).

Steel	CSR (pct)	CLR (mm/cm2)	CTR (pct)
AB	0.29 ± 0.16	0.52 ± 0.22	2.3 ± 1.2
AE	2.35 ± 0.58	5.20 ± 0.86	7.5 ± 1.5
AG	0.12 ± 0.11	0.26 ± 0.21	0.7 ± 0.4
CA	1.64 ± 0.54	2.96 ± 0.53	12.9 ± 2.8
CB	4.64 ± 0.87	7.20 ± 0.89	17.0 ± 2.5
CC	0.28 ± 0.09	1.54 ± 0.35	3.0 ± 0.8
CD	0	0	0
CE	0.03 ± 0.03	0.08 ± 0.07	0.2 ± 0.2
Z	0.75 ± 0.45	1.90 ± 0.48	3.9 ± 1.4

Table 4 - Quantitative measurements of inclusion distributions.

Pipe	Total Inclusion Length mm/cm^2	Area fraction of Inclusions pct.
AB	97.1 ± 2.1	1.08 ± 0.06
AE	10.6 ± 1.5	0.22 ± 0.03
AG	7.8 ± 2.0	0.12 ± 0.02
CA	95.6 ± 9.6	1.50 ± 0.20
CB	153.7 ± 25.0	2.45 ± 0.75
CC	33.1 ± 5.1	0.23 ± 0.03
CD	103.7 ± 2.4	1.09 ± 0.05
CE	6.3 ± 1.2	0.17 ± 0.03
Z	60.5 ± 7.5	0.80 ± 0.26

A2.

Fig. 1. Typical example of SWC (steel CB.) X50 (neg 5014)

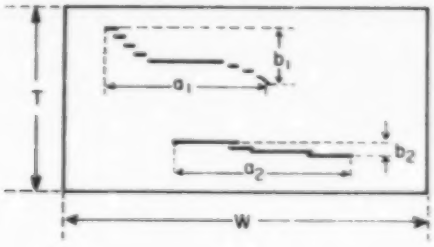

$$\text{Crack Sensitivity Ratio (CSR)} = \frac{\sum a \times b}{W \times T} \times 100\%$$

$$\text{Crack Length Ratio (CLR)} = \frac{\sum a}{W} \times 100\%$$

$$\text{Crack Thickness Ratio (CTR)} = \frac{\sum b}{T} \times 100\%$$

Fig. 2. Definitions of quantities used to evaluate SWC. (neg 4140)

A2.

IMAGE MANIPULATION

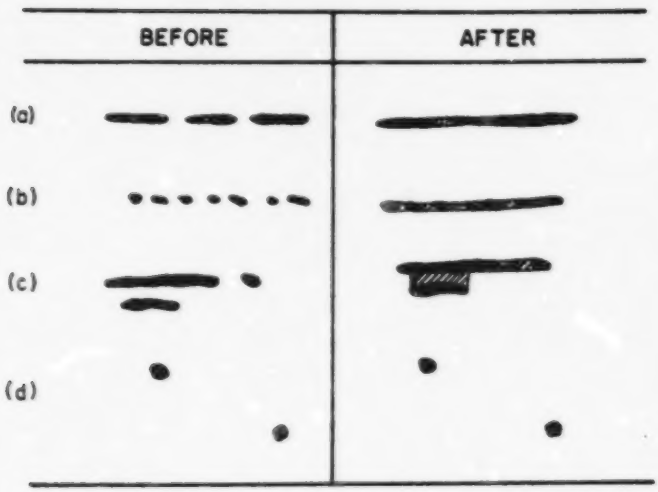

Fig. 3. Image manipulation by dilation and erosion of inclusion images. (a) broken sulphide stringer (b) planar array of angular or ellipsoidal particles (c) adjacent stringers (d) dispersed particles. (neg 10750)

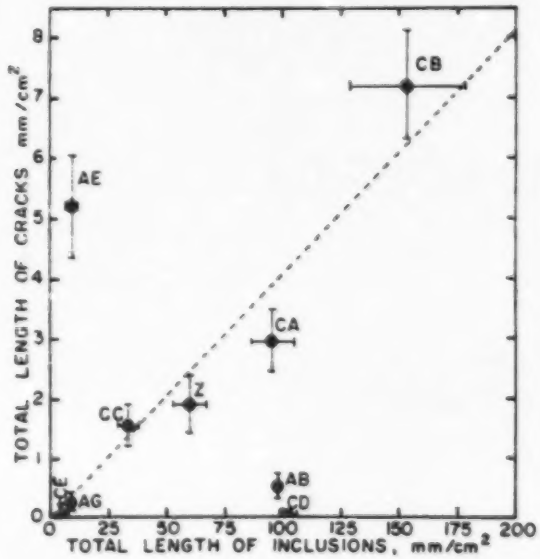

Fig. 4. Correlation between total length of inclusions per unit area and CLR. (neg 10798)

A2.

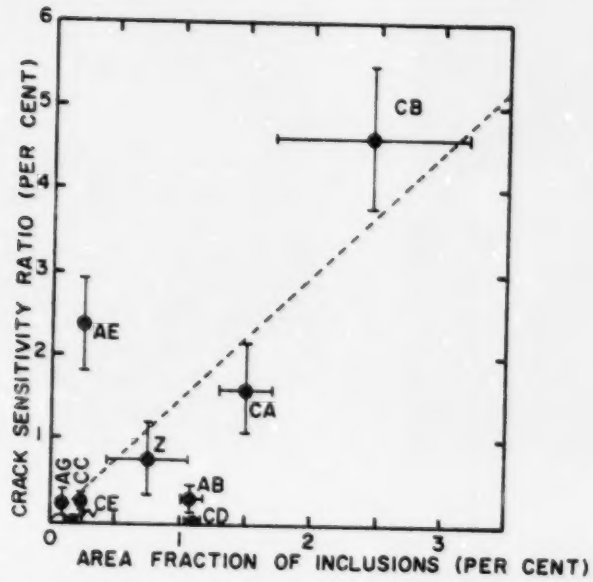

Fig. 5. Correlation between area fraction of inclusions and CSR. (neg 10797)

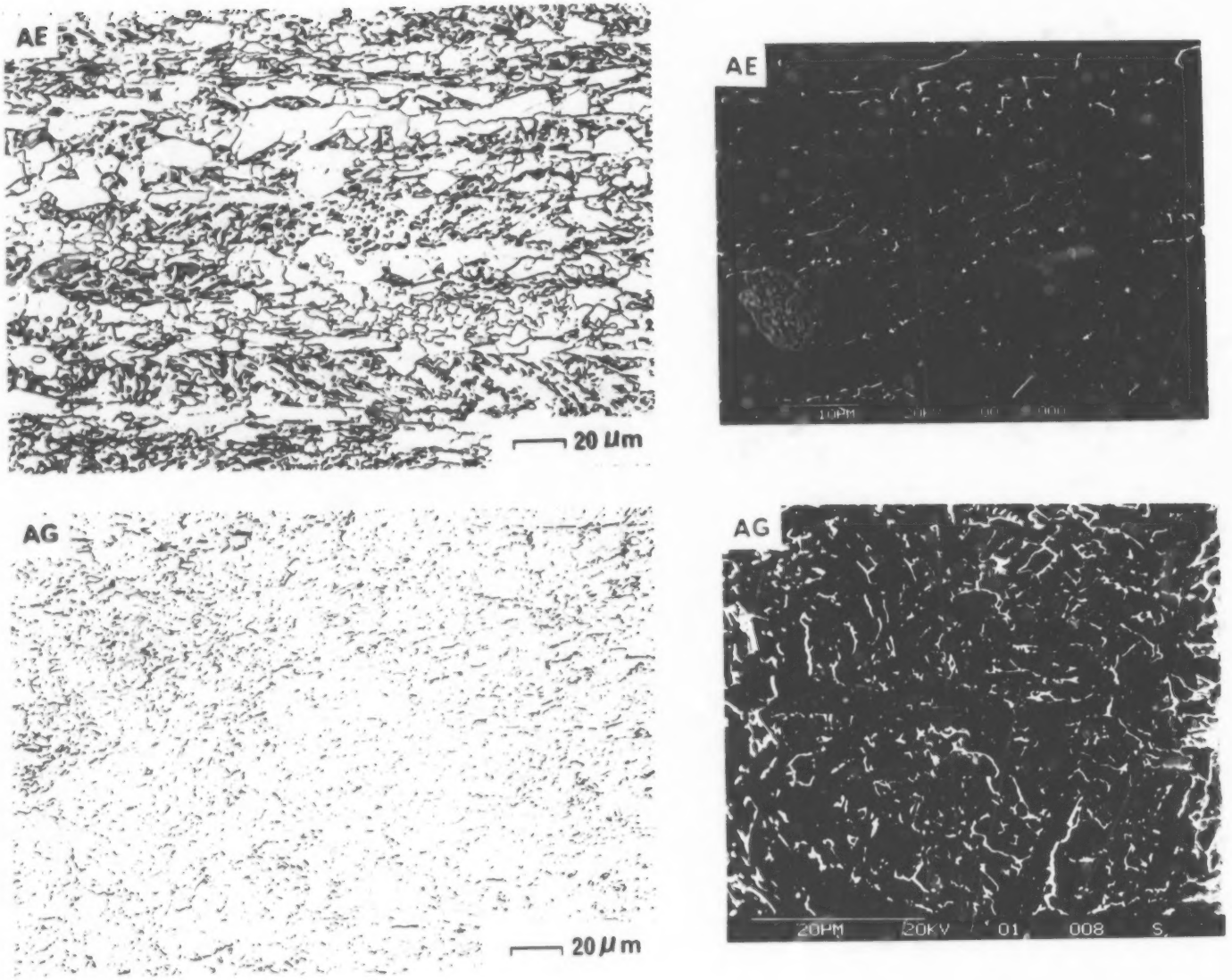

Fig. 6. Microstructures of steels AE and AG, optical (L) and SEM (R). (neg 10749)